EXPERIMENTAL STUDY OF CLAST ORIENTATION IN GRAVELS DEPOSITED BY UNIDIRECTIONAL FLOW

by

James G. Danna

Bachelor of Science

SUBMITTED TO THE DEPARTMENT OF EARTH, ATMOSPHERIC, AND PLANETARY SCIENCES IN PARTIAL FULFILLMENT OF THE REQUIREMENTS FOR THE DEGREE OF

MASTER OF SCIENCE

at the

MASSACHUSETTS INSTITUTE OF TECHNOLOGY

September 1985

Signature of Author _____
Department of Earth, Atmospheric, and Planetary Sciences
September 6, 1985

Certified by _____
Professor John B. Southard
Thesis Supervisor

Accepted by _____
Theodore R. Madden
Chairman, Graduate Thesis Committee

EXPERIMENTAL STUDY OF CLAST ORIENTATION IN GRAVELS DEPOSITED BY UNIDIRECTIONAL FLOW

by

James G. Danna

Submitted to the Department of Earth, Atmospheric, and Planetary Sciences on September 6, 1985 in partial fulfillment of the requirements for the degree of Master of Science.

Abstract

A series of experimental runs were conducted under controlled laboratory conditions to investigate the fabric of gravel deposits formed under a range of flow strengths and sediment discharges. A closed-circuit recirculating flow duct, specially constructed for the research, was designed to produce strong flows and to transport large (up to 6 cm) clasts in concentrations as high as possible.

The sediment used had a median grain size of 8.57 mm and was coarse-skewed. The clasts were generally well rounded and were predominantly disks and blades. The water discharges used ranged from 0.024 m^3/s to 0.054 m^3/s, producing flow velocities in the main flow duct from 1.45 m/s up to 2.65 m/s. Sediment discharge per unit width was varied from 2.6 kg/s-m up to 39.5 kg/s-m. The deposit was formed by lowering a false floor within the main flow duct, and the fabric of the deposit was quantitatively analyzed by measuring the spatial orientation of 100 to 340 of the larger clasts in a deposit for each run. An analysis of the grain-size distribution was also made.

As flow strength increased, fewer large clasts were deposited, producing a bed of predominantly fine material. Increasing flow strength also resulted in a stronger preference of a clast A-axis orientation parallel to the flow direction. By separating the clasts of a run into shape and size groups, and comparing the orientation distributions, it was found that rods were more influenced by changes in flow conditions than were blades or disks. No definite variations were found between size groups.

Thesis Supervisor: Professor John B. Southard
Title: Associate Professor of Geology

Dedication

This work is dedicated to my mother and father, whose unending love and guidance have always helped me to succeed.

Acknowledgements

A great many people have helped me during all stages of work that led to the successful completion of this thesis. Thanks go to all the undergraduate employees that spent many hours working with me over the last two years, from the start of construction to the last clast measurement. I would also like to thank all my friends that were always there for moral support.

The assistance given to me by Sarah Saltzer with the computer plotting programs is greatly appreciated. I am grateful for the help I received from Joe Cerutti, Scott Stull, and Douglas Southard with the demanding task of sediment feeding.

I also extend many thanks to Judith Stein for her work in the administrative areas, and for being able to make it all balance in the end.

Doug Walker provided a lot of guidance with construction problems, as well as assistance with ways to approach the actual experimention and obtain results. And Dave Milich spent time creating several programs that greatly simplified the manipulation of the data, showing me that a computer is my friend.

I will always be indebted to Ellen Epstein and Lei Tung for all their help in putting this together in the final frantic moments. No matter how much I thank them, it won't be enough.

My fellow researchers, Roger Kuhnle and Peter Wilcock, also cannot be thanked enough. They have helped me all the way with all aspects of the project, and kept me moving when I slowed down.

And, of course, I am very grateful to Prof. John Southard for the opportunity to carry out this study. I have learned a great deal from John, not just about sedimentology and science, but about all the skills necessary to complete this project. His enthusiasm and creativity were also indispensible.

The greatest thanks go to my parents, Mary and Alfred Danna. They have always given me every opportunity to pursue what I thought was right for me, and always provided the support and encouragement that I needed during my college career and all my life.

Table of Contents

List of Figures

List of Tables

Chapter 1
Introduction

Fabric, as defined by the preferred orientation of clasts, is a very important but not very well understood feature of gravels and conglomerates. As pointed out by Harms (1975), this fabric may provide the necessary clues to determine the modes of transport and deposition of conglomerates that lack sedimentary structures. If understood, the presence of preferred clast orientation also reveals information about direction, strength, uniformity, and sediment concentration in the paleoflow. From these it may be possible to develop a model for the depositional environment.

The orientation of a clast is defined by the the trend and plunge of the A axis (longest axis) and the strike and dip of the AB plane (the plane of maximum projection, containing the A axis and the B axis). Often the trend and plunge of the C axis (shortest axis) are used, the C axis being the pole of the AB plane. Numerous authors have described clast orientation in the field. Both Walker (1975) and Johansson (1965) present extensive literature reviews of studies which describe the existence of preferred clast orientation. Through the compilation

of the information, similar trends were found in similar depositional settings and conclusions were drawn from these. It was conceded, however, that experimental work is lacking in this area, and such work would be of great value in interpreting fabric under more controlled conditions than are found in the field. Koster (1977) attributes part of the lack of laboratory study to the demands that the transport of coarse gravel make on equipment.

The present study was conducted with two primary goals. The first was the design of an apparatus tailored to meet the requirements necessary to produce controllable unidirectional high-velocity flows transporting various concentrations of coarse gravel, and to allow the generation and analysis of a deposit from these flows. This apparatus would allow the relatively unexplored area of high-velocity coarse-sediment flows to be opened to experimental investigation.

The second aim was to conduct a survey of the basic factors controlling the orientation of clasts deposited by these flows under a range of conditions, so that direction may be given to further areas of study. Although not quite as broad in scope as originally intended, the range of experimental conditions achieved was much wider, and involved much stronger flows than those used in laboratory work previous to this study, with satisfying results.

Grain-size distributions of deposited material were obtained and compared with those of the transport load. Several interesting fabric characteristics and bed structures were produced and described. The bulk of the work, however, was the extensive measurement of clast orientations in the deposits. These data were combined to produce an overall orientation preference for each experimental run. Also, for a given run, they were divided into shape and size groups, so that variations in orientation with shape or size could be examined. Through this controlled process, factors influencing clast fabric and conditions that produce a particular fabric can be determined.

Chapter 2

Review of Previous Work

Davies and Walker (1974) conducted an extensive analysis of the clast fabric of the Cap Enragé Formation, a resedimented conglomerate in Gaspé, Quebec, as part of a study to construct a facies model for the deposition of resedimented conglomerates. The A-axis orientations of 6900 elongated clasts and a smaller number of C-axis orientations were measured in 89 localities throughout the formation. The study showed a mean dip of the AB plane of 12 deg (with a standard deviation of 10 deg) in a northeastward direction, suggesting a paleoflow direction towards the southwest. The vector mean of the A axis orientations was southwesterly at 236 deg (with a standard deviation of 10 deg). Davies and Walker concluded that there was a strong preferred orientation of the A axes in the direction of flow.

Hendry (1976) made a similar study of the fabric of resedimented conglomerates of the Cap des Rosiers Formation, also in Quebec. Hendry measured the degree and direction of dip of the AB planes of disk-shaped clasts, and found a weak but consistent preferred orientation described by the direction of dip of the planes.

Sedimentary structures in the formation (several flute marks in the conglomerate and ripple marks and cross-stratification in sandstone beds of the same formation) indicated that as the plane dipped in the upstream direction of the paleoflow. Hendry concluded that the fabric preserved in the conglomerate beds reflected transport and deposition, as well as postdepositional processes.

Krumbein (1939) made a comparative study of A-axis and C-axis orientations of pebbles from a glacial till, an outwash terrace, and a beach, describing in great detail methods for the graphical and statistical analysis of the data. From measurements of 100 pebbles from a late Wisconsin outwash terrace in Illinois, Krumbein found a weak flow-parallel A-axis orientation, and a weak upstream imbrication of the AB plane (normal to the C axis). He suggested that variations in flow velocity and shape are responsible for the wide scatter, as well as varying depositional modes for clasts of different sizes (tractional deposition for the larger clasts, deposition from suspension for the smaller).

Studies of modern deposits afford the researcher the opportunity to ascertain first-hand the flow conditions under which the deposit was formed. Lane and Carlson (1954) published the results of a study of the gravel beds of canals at eighteen test sections in southern Colorado.

The flow velocities at the sections varied from 0.4 m/s to nearly 2.0 m/s. Detailed measurement of clast orientation, as well as axis length and clast weight of the bed material, were taken, and the Zingg shape, sphericity, and roundness of the clasts were measured. They found a definite overall trend of A axes transverse to flow, attributing this to tractional transport. They also found that disk-shaped clasts were less easily transported than equant clasts.

The fabric of two small gravel bars in Wolf Run, a modern stream in Indiana, which were deposited by high-velocity, turbulent flood waters, were studied by The Sedimentary Petrology Seminar (1965). The azimuths and dips of the AB planes And the A axes of nearly 300 clasts were measured. The results showed a median upstream dip of the AB plane of 23.3 deg, with the mean orientation of the dip direction deviating only 6 deg from the known flow direction. The A axes showed a preferred orientation transverse to the flow direction.

Rust (1972a) also found a preferred A-transverse orientation in a study of a glacier-fed river bed in Canada. Analysis of almost 1500 clasts ranging in size from less than 5 cm up to 30 cm measured at 23 locations also showed a well defined upstream dip of the AB plane. Rust also discussed the effects of size and shape, and suggested a decrease in preference of A-transverse

orientation with increasing clast concentration and size, but cautioned that the nature of the deposit should be carefully considered when using information on clast orientation to determine paleoflow characterstics.

Most of the experimental work done with gravels has involved the transport of large clasts on a sand bed. Johansson (1963) conducted a study of the transport of pebbles on the topset and foreset beds of an artificially produced delta-like sand bed. He observed a definite A-transverse orientation on the level topset bed, but as the clast reached the foreset bed, the orientation became more erratic and the velocity of the grain increased, being transported by gravity.

Kelling and Williams (1967) studied the reorientation of pebbles and shells on a sand bed in a flume. It has been suggested that the orientation of a clast may reflect its transport or depositional mode, but it may actually be a response to the stresses exerted on it by the flow after downstream movement has ceased. Kelling and Williams found that the shift in orientation of a clast is primarily a function of flow velocity, with Zingg shape, roundness, and sphericity having a lesser effect.

Chapter 3
Equipment and Sediment

3.1 System Layout

The principal apparatus used for these experiments was a closed-circuit recirculating flow duct (Fig. 3-1) designed and constructed to handle the high-velocity, high-concentration, coarse-sediment flows required. Water and sediment were drawn out of an elevated mixing tank by a centrifugal pump, and driven through a 4.96 m long horizontal duct with a constant 6" x 6" (0.15 m x 0.15 m) cross section, consisting of a 3.66 m steel approach section and a 1.28 m deposition section. Upon leaving the chamber, the flow then made a 180 deg turn and entered a large closed collection box. A large decrease in flow velocity accompanied the sudden flow expansion, resulting in deposition of the gravel in the box. The water passed out of the box through a return pipe and back into the mixing tank to be recirculated.

The mixing tank was constructed by fitting a frame of 3" x 3" x 3/8" (76 mm x 76 mm x 9.5 mm) steel angle with panels of 1" (25 mm) plywood. The tank was open at the top, and had inner dimmensions of 54" x 48" x 33" (1.37 m

A - Mixing Tank

B - Pump and Motor

C - Primary Valve

D - Bypass Line

E - Duct: Approach Section

F - Low-feed Standpipe

G - Duct: Depostion Section

H - Collection Box

I - Return Pipe

J - Overflow Tank

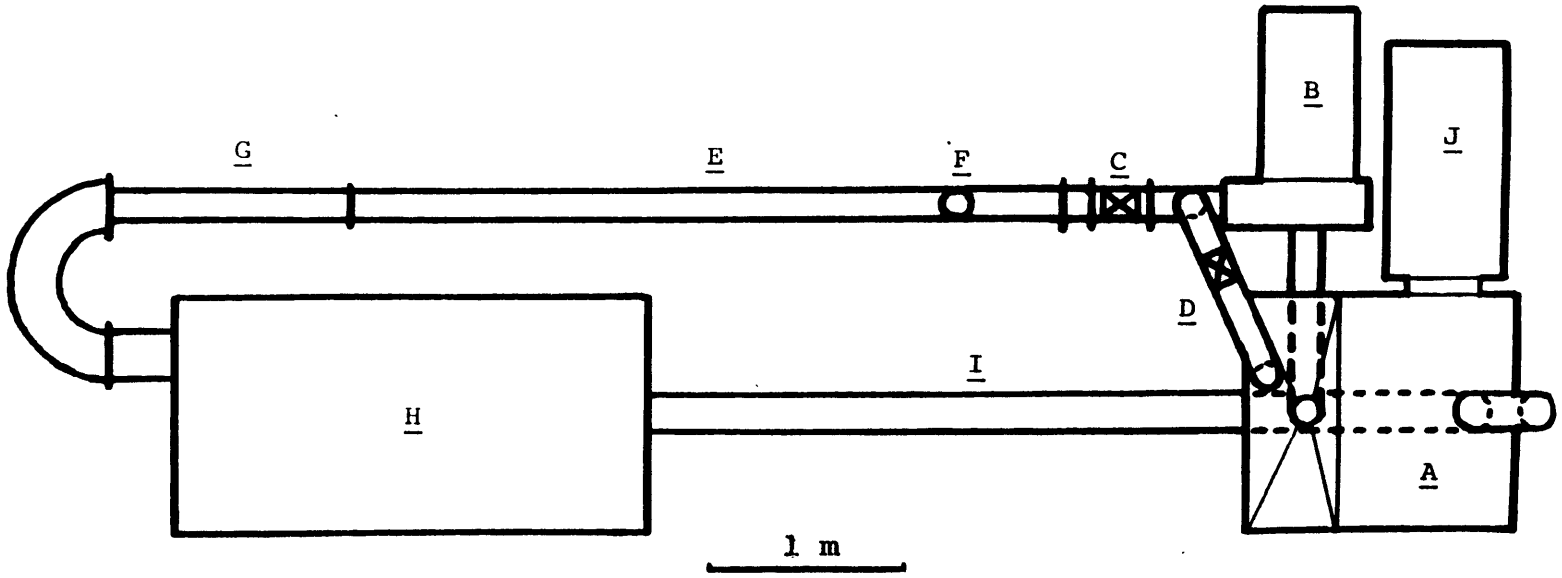

Figure 3-1: Plan View of Experimental Apparatus

x 1.22 m x 0.84 mm). To make the tank watertight, the inside seams were sealed with 6" (0.15 m) strips of fiberglass cloth tape, and the entire tank was coated with several layers of polyester resin. The box was placed on a steel frame, raising it 36" (0.91 m) above the floor. The 6" (0.15 m) exit port from the mixing tank was located in the floor of the tank, 0.31 m from the downstream side. Resin-coated 1" (25 mm) plywood panels were used to form a funnel inside the tank to direct the gravel towards the exit.

The gravel and water were drawn into the pump from the mixing tank through a 6" (0.15 m) steel elbow attached to the tank exit. The procedure for sediment feeding will be described in more detail in a later section. Since the pump entrance was located below the level of the mixing tank, a negative suction head was eliminated. The pump was a Denver 6" x 6" (0.15 m x 0.15 m) soft-rubber-lined (SRL) centrifugal slurry pump, belt-driven by a 40-hp 3-phase induction motor. This pump was selected because it could accommodate the greatest discharge of water and sediment that might be desired. Slurries of up to 70 percent solids with clast sizes up to about 65 mm could be pumped, although much lower concentrations were used in these experiments. Discharges up to almost 0.1 m^3/s (about 1500 gpm) were attained in calibration runs with this pump and this system.

To increase the life of the packing gland of the slurry pump, clear flush water was forced into the pump through the gland by a high-pressure, low-discharge positive-displacement screw pump. The discharge of flush water pumped into the system was about 9 gpm, and was included in the system discharge measurements.

At the upstream end of the duct was the primary flow regulator, a 6" (0.15 m) gate valve. This gate valve originally was to be connected to the pump exit by a 0.38 m straight length of 6" (0.15 m) steel pipe. It was discovered, however, that the flow could not be sufficiently reduced to the desired discharge ranges with this valve alone, since the valve had to be open a minimum of about 65 mm to allow the gravel to pass. The length of straight pipe was therefore replaced by a steel tee, and a 6" diameter (0.15 m) bypass line was installed to reroute part of the flow back into the mixing tank. This allowed the primary valve to be opened more widely while still attaining the lower flow rates. The flow through the bypass line was controlled by a separate 6" (0.15m) gate valve. (The bypass line delivered the rerouted flow into the mixing tank directly above the exit port of the mixing tank, so that any sediment entrained in this flow would reenter the main flow immediately, and not be removed from the system by deposition in the rear of the mixing tank.)

After several runs it was decided that the flow rates

required were lower than those possible even with the primary valve closed down to the minimum allowable opening and the bypass valve full open. Since the limiting factor was the necessity for gravel to pass through the primary valve, the problem was circumvented by attaching a 1.8 m removable vertical standpipe to the top of the approach section of the duct just 0.7 m downstream of the primary valve. For low-discharge runs the primary valve could be closed down to the necessary conditions, and the sediment fed through the standpipe. For high-discharge runs the standpipe could be removed. Head loss in the duct was such that the maximum discharge possible without the standpipe overflowing was very near the minimum discharge attainable with sediment passing through the main valve.

The 3.66 m approach duct was connected at its downstream end to the heart of the system, the deposition section, shown in the photo in Figure 3-2. The flow geometry remained constant through the transition. The deposition section, 1.28 m long, constructed from sheets of clear acrylic plastic, had inner dimensions of 1.22 m x 0.61 m x 0.15 m. Square holes to match the inner dimensions of the square duct were cut in the upstream and downstream walls of the section, and acrylic flanges were attached so that the section could be slipped into the line between the approach duct and the return bend. A lid was attached by bolting it to a steel flange that was

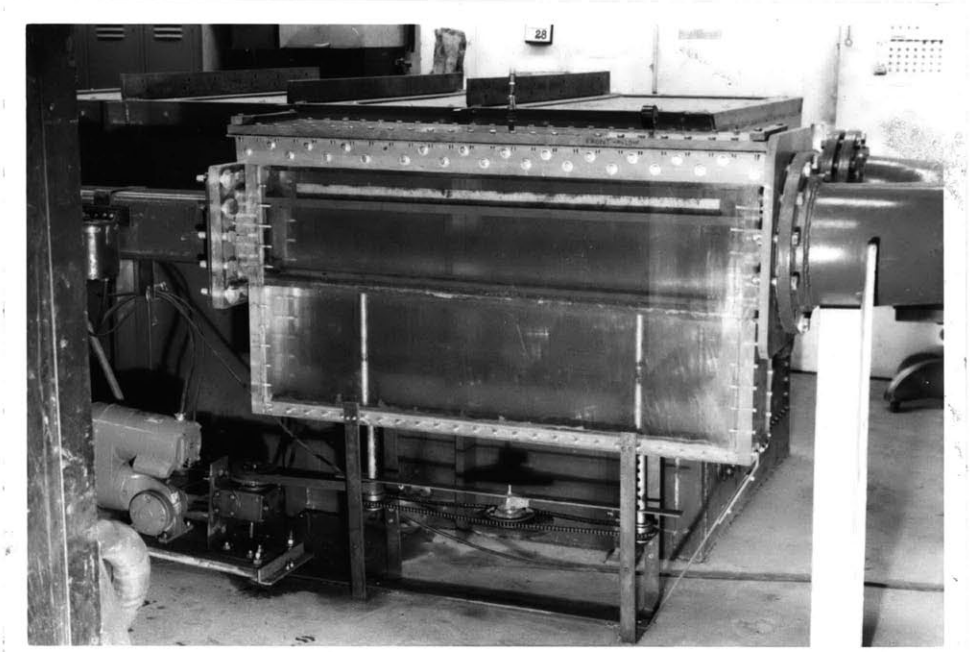

Figure 3-2: Deposition Section of Flow Duct

fixed to the top outer edges of the section. The lid was removable to permit access to the inside, and was resealed prior to each run with silicone rubber caulk. The inside seams of the section were permanantly sealed with the same caulk. The lid was fitted with a bleed valve to remove air that tended to collect in the chamber during a run or during filling of the system with water before a run, and a drain valve was located near the floor. For safety purposes, a removable steel girdle surrounded the section to minimize the bulging of the large side panels during high-discharge runs.

Inside the deposition section a removable false ceiling was installed so that the upper boundary of flow was coplanar with that of the duct upstream. The floor, however, was not fixed, but instead was designed so that it could be raised or lowered at any time before, during, or after a run. This was done by attaching the floor to two vertical 3/4" (19 mm) aluminum shafts that passed through the floor of the chamber. Rubber O-ring seals kept the chamber watertight while allowing the shafts to move vertically. Outside the chamber the shafts were each connected to two vertical 9" (0.23 m) lengths of threaded rod. Each rod and shaft assembly was forced to move vertically by rotating a nut threaded onto the rod, the steel nut being held at a fixed height above the lab floor.

A sprocket was welded to each nut, and the two nut-sprocket units were coupled by a length of roller chain, so that the the two aluminum shafts were moved in unison. This entire drive system was linked by a series of speed-reducing belts to a 1.5 hp variable-speed gear motor controlled by a forward-stop-reverse switch, so that the shaft assemblies, and ultimately the false floor, could be raised or lowered at an adjustable rate to suit the various run conditions. The drive system was calibrated at the start of the experimental program so that the descent rate of the inner floor was known for any motor setting.

Upon leaving the deposition chamber, the flow, carrying the sediment not deposited in the chamber, passed through a 180 deg steel-pipe bend and into the collection box. This box, 4' x 4' x 8' (1.22 m x 1.22 m x 2.44 m), was similar in construction to the mixing tank, having a steel frame and 1" (25 mm) resin-coated plywood walls. These walls were reinforced on the outside with heavy steel bars welded to the steel frame, to eliminate bulging. The upstream wall, however, consisted not of plywood but of 1/4" (6.4 mm) steel plate. A 0.61 m x 0.76 m rectangular hole was cut in this plate, about 0.25 m from the bottom, and was fitted with a 1/4" (6.4 mm) steel plate that could be bolted tightly over the hole. This lid was sealed with a 1/4" (6.4 mm) rubber gasket. The

180 deg bend was connected to the collection box by means of a flanged 8" (0.20 m) steel pipe 0.24 m long which was welded to the upper corner of the upstream panel of the box. The main drain valve for the system was a 2" (51 mm) gate valve located near the downstream end of the box. Also, a bleed valve similar to that installed in the lid of the deposition chamber was installed in the top surface of the collection box to prevent buildup of air.

Because of the increase in cross-sectional area from the bend to the collection box, the velocity of the flow, as well as its competence, decreased sharply, resulting in deposition of the transported sediment in the box. To promote deposition near the upstream end of the box, where it could be removed more easily, a 0.3 m x 0.3 m deflecting plate was attached to the inside of the steel wall 0.2 m in front of the entrance of the box to break the flow. In addition, a partition 0.76 m high and spanning the inner width of of the box was installed on the floor of the box 0.6 m from the downstream wall to prevent sediment from reaching the exit of the box.

Free of all but a minor proportion of the finest sediment size fractions, the flow left the collection box through a horizontal 8" (0.20 m) return pipe 4.6 m long just above floor level and then vertically upward through 1.8 m of similar pipe, and into the open top of the mixing tank through a 180 deg miter bend near the rear of the

tank (farthest from the tank outlet). The water in the tank was very turbulent, and in early trials a great deal of air was entrained in the flow. After several unsuccessful attempts to eliminate or reduce this air entrainment, it was found that a partition separating the upstream part of the tank from the downstream part, over which the water had to pass to reach the outlet on the bottom, worked the best.

To accommodate the volume of water that was displaced by feeding sediment into the already-full system during a run, an overflow tank, similar in construction to the mixing tank and the collection box, was built. The tank was 0.6 m x 1.2 m in horizontal cross section and 1.8 m high, the same height as the upper edge of the mixing tank, and was connected to the mixing tank by a rubber-lined spillway. The displaced water flowed freely over the spillway and into the overflow tank as sediment was added during a run, and the tank was drained afterward by a valve at the bottom of the tank.

Water discharge was measured during each run using a bend meter and a U-tube liquid-liquid manometer. Two pressure taps were located on the inside of the 90 deg miter bend that connected the horizontal and vertical sections of return pipe downstream of the collection box, where the flow was mostly free of sediment. The meter was calibrated by measuring the volume of water discharged in

a given period of time over a range of flow conditions. This calibration was carried out before making any runs with sediment.

3.2 Sediment

Considerable thought was given to the selection of the sediment to be used in the experiments. It was thought that rounded clasts of regular and readily definable shapes (spheres, rods, disks, and blades; Zingg, 1935) and easily measured principal axes would show the features of the fabric of a deposit best, and simplify the task of measuring the orientations of the A axes and the AB planes of the clasts. A survey of several beaches in southeastern New England during the winter months led to the location of two beaches that together provided sediment suitable for to use in these experiments.

The first source of sediment was the Scituate Town Beach, on the south shore of Massachusetts Bay. The beach deposits there are of pebble to small cobble size, well rounded, and mostly discoidal but with some elongated and bladed clasts as well. About 1150 kg (2500 lb) of sediment with clasts ranging in size from 4 mm to greater than 32 mm (sieve diameter) was collected from this beach. About 90 percent of the gravel collected was between 8 mm and 32 mm in size. The second source of sediment was the shoreline of Brenton Point State Park in Newport, Rhode

Island. This beach is mostly sandy gravel, the clast shapes in the gravel being mostly bladed. The grain size ranges from less than 0.5 mm to 32 mm, with a mean size between 2 mm and 4 mm. Another 1150 kg (2500 lb) was collected here.

Processing of the sediment was very time-consuming. The Scituate gravel was sieved into batches with whole-phi intervals and stored. The size fractions less than 1 mm and greater than 32 mm were removed from the Newport sediment by wet-sieving, and portions from the various size batches of the Scituate gravel were then added to the Newport base to obtain the desired composite grain-size distribution. A log-normal distribution was originally tried, but a trial run using this mix produced a deposit that was seriously deficient in the coarser clast sizes (greater than 15 mm).

After several more trials with different size distributions, a sediment mix was developed that produced suitable deposits under the range of flow conditions used. The cumulative size distribution curve of this sediment mix is shown in Figure 3-3. The graphical mean (Folk and Ward, 1957) of this distribution is -2.85 phi (7.24 mm), with a standard deviation of 1.92 phi. The median size is -3.10 phi (8.57 mm). The distribution is significantly skewed towards the coarser sizes (Inclusive Graphical Skewness = 0.24, Folk and Ward, 1957) due to the large

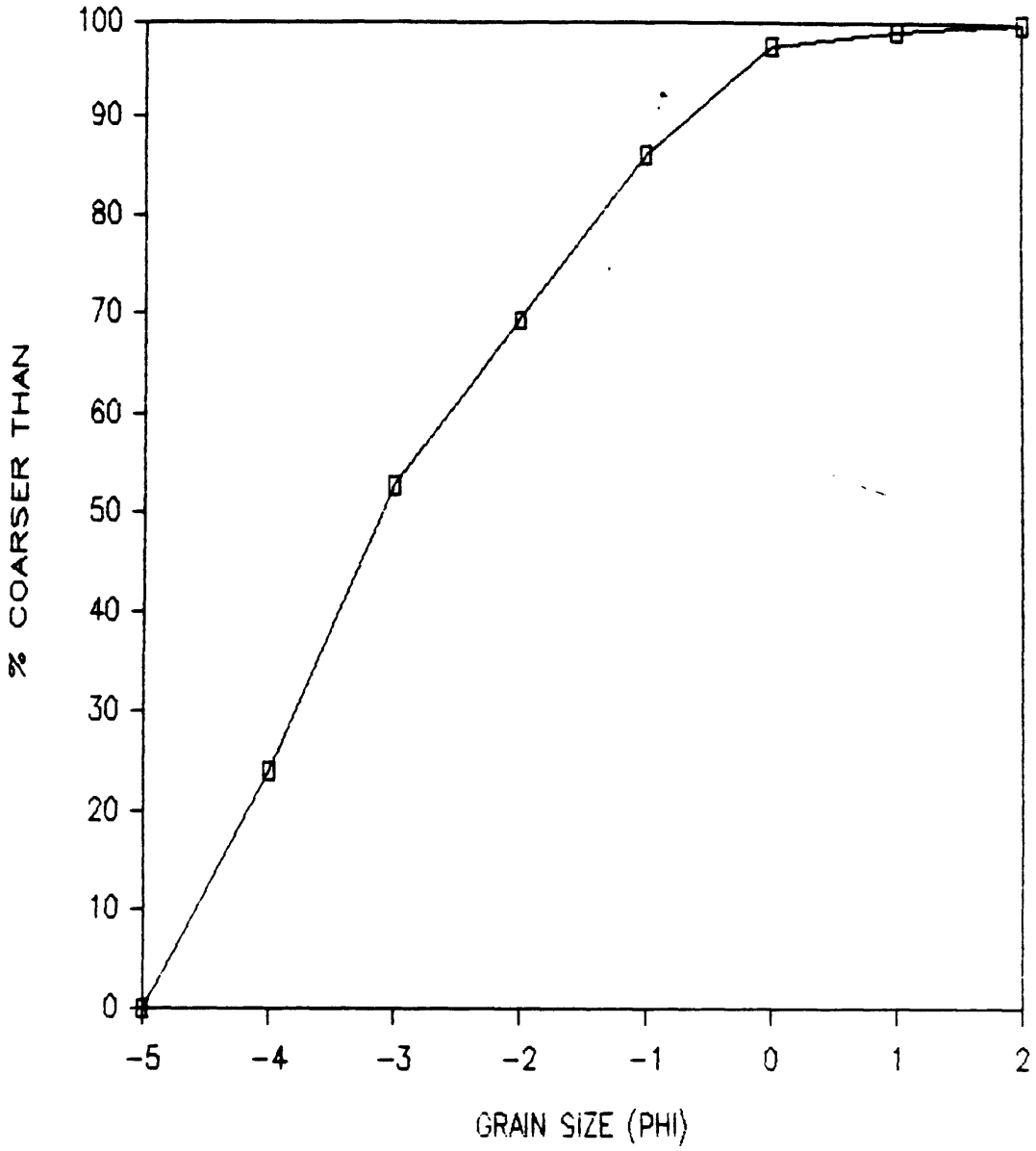

Figure 3-3: Cumulative Size-Distibution Curve of the Sediment Feed Mix

percentage of coarse clasts (greater than 8 mm) that had to be added to the originally log-normal mix.

Many previous studies of clast orientation in gravel deposits suggest that clast shape and size play an important role in the development of a preferred orientation. A quantitative method of describing the distribution of clast shapes of was therefore desired. A sample of the well mixed sediment was taken, and all clasts with an A-axis length of 15 mm or more were collected from the sample, the final population numbering 405. The lengths of the three principal axes of the grains were measured in a manner similar to that described by Griffiths (1957), the three axes being mutually perpendicular but not necessarily intersecting at a common point. A measuring device was used that consisted of two 20 mm high blocks about 80 mm long attached perpendicular to each other on a 15 cm square wooden base on which graph paper with millimeter spacing had been laid. The clast was placed within the right angle formed by the two blocks with its A axis parallel to one block and the B axis parallel to the other. The lengths of the A and the B axes were read visually, using the graph paper grids as a scale. The clast was then rotated 90 deg about the A axis so that the C axis was parallel to the base and its length could be determined in a similar manner. The shape classification system employed was that proposed by Zingg

(1935), and was based on two indices: the B:A ratio and the C:B ratio. All possible combinations of these ratios can be plotted on a square grid, the ratios ranging from zero to one. Zingg divided this grid into four regions, each region defining a shape. The results of the shape study are shown in Figure 3-4. It is obvious that there is a predominance of disk-shaped and blade-shaped clasts, due to the nature of the sediment originally chosen.

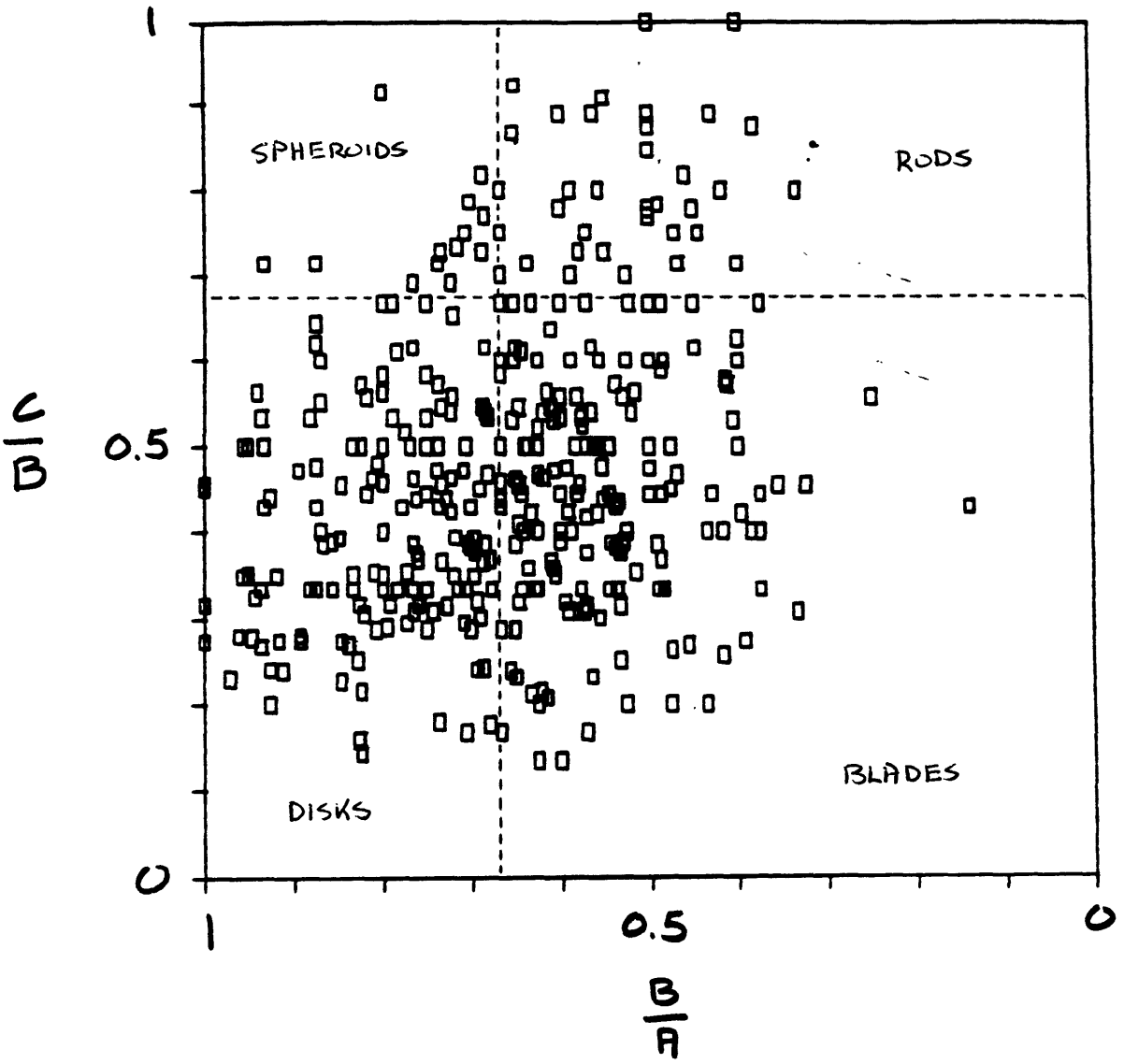

Figure 3-4: Distribution of Sediment Feed Mix by Zingg Shape Classification

Chapter 4
Experimental Procedures

4.1 Sediment Feeding

The high sediment transport rates in some of the runs necessitated a sediment feeding method that permitted a large volume of sediment (6.0 kg/s; 13.2 lb/s) to be introduced into the system at a rapid rate and as uniformly as possible. The sediment feed rate had to be adjustable for the varying flow conditions, but any automatic sediment-feed device used had to be free of the tendency for large clasts to jam in the feed aperture. Originally, a triangular hopper with an adjustable gate that would allow the sediment to flow into the mixing tank under its own weight was constructed. After several trials, however, this hopper proved unsatisfactory, largely because the shape and position of the hopper were not ideal owing to lack of sufficient headroom in the laboratory. Instead, a more labor-intensive but more controllable method was used: sediment was fed manually into the mixing tank using standard #10 metal food cans as a unit volume, each can holding 6 kg of sediment. (This turned out to be a very managable unit size, since a

greater weight would have tired the sediment feeders too quickly, and a smaller volume would have required too much handling time.)

Depending on the sediment feed rate required for a particular run, one to three assistants poured the sediment, can by can, into the mixing tank, directly above the tank exit, in a regular alteration. Each feeder overlapped the previous feeder, to minimize pulsing. The pace was maintained by a timekeeper, who shouted for the next feeder to begin. The maximum sustainable rate at which one person could feed sediment was one can every three seconds, and three persons feeding during a run was the most possible due to space limitations, resulting in a maximum total feed rate of one can per second, or 6 kg/s. These high-discharge runs were a hectic, noisy, communal affair, but the feeding was very effective. Higher rates were within the capability of the pump, but could have been attained only by construction of an entirely different automatic system, like a large preloaded conveyer belt. But there was insufficient time for the arrangement of such a new system.

As mentioned earlier, the lower discharges in some of the runs required that the sediment be introduced into the system through the standpipe downstream of the primary valve. Because of the lower feed rates (less than 1 kg/s), only one feeder was needed, with the cans being

passed to him by the timekeeper. The sediment was poured into a funnel-shaped attachment at the top of the standpipe as uniformly over the time interval as possible, again to eliminate pulsing.

4.2 Preliminary Runs

Before any official runs could be made it was necessary to ascertain by preliminary runs the equilibrium combinations of water discharge and sediment feed rate that would result in a sediment bed of desired thickness in the steel duct and the deposition chamber. If the water discharge was too great for a given feed rate, no deposit would form; if the water discharge was too low, the duct would tend to plug. A bed thickness of 30 mm to 50 mm was chosen. Originally expected to be a very time-consuming trial-and-error process, the set of desired combinations was actually determined fairly easily.

Before a particular preliminary run, a sediment feed rate was chosen. The system was filled with water, and, with the primary valve nearly closed, the main and auxiliary pumps were started. (The pumps were always started with the primary valve nearly closed, to avoid a sudden pressure surge in the deposition chamber.) The primary valve was then opened full, and the sediment was fed into the system. The primary valve was slowly closed down until a bed of the desired thickness had formed in

the deposition chamber. (The inner floor of the chamber remained stationary during these preliminary runs.) When it was determined that the bed was neither aggrading nor degrading, the sediment feed was stopped and the system was shut down.

During each preliminary run, manometer readings were taken at regular time intervals, so that a mean discharge could be calculated and associated with the given sediment feed rate. This was done for each feed rate to be used; no interpolation was necessary to obtain the equilibrium conditions.

4.3 Official Runs

Once the preliminary runs were completed and the set of flow-rate and feed-rate conditions established, official runs could be made and data collected. Prior to each run the sediment was thoroughly mixed in two large, shallow bins and the sediment cans were filled and loaded into place on several platforms set up adjacent to the mixing tank, positioned so that they could be reached by the feeders without assistance. The lids of both the collection box and the deposition section were sealed, and the bleed lines opened. The system was filled with water to capacity (until the water spilled over from the mixing tank into the overflow box).

Once having predetermined the sediment feed rate that

was to be used during the run, the length of the running time could be calculated, being limited by the volume of sediment. (For the two slower runs there were more than enough filled cans.) Allowing the first 30 to 60 seconds of running time for a bed to form in the approach and deposition sections, the time available for lowering the inner floor of the deposition section and building a deposit was calculated, and the motor speed adjusted to build a deposit 0.18 m - 0.20 m thick in this time.

With the sediment in place, the system filled with water, and the floor-lowering rate set, the official run was begun. The main and auxiliary pumps were started and the primary valve was adjusted to obtain the desired flow rate. The sediment feeding was started, and manometer readings were taken at regular intervals (3-15 seconds, depending on the feed rate). The flow was observed through the walls of the deposition section, noting any irregularities or special features. When the equilibrium bed was established in the duct, the motor was turned on and the floor lowered until the deposit was built. The bed surface was carefully watched during this time to be sure the floor was not lowering at too fast a rate, which would result in development of a delta at the upstream end of the deposition chamber. The flow depth, measured from the false ceiling to the bed, was then recorded. When the deposit was fully formed, the floor and the sediment feed

were stopped and the pumps were shut off. The system was drained, and the deposition section and the collection box opened. The sediment was shoveled from the collection box and back into the bins to be remixed for the next run, and the deposit was ready to be measured.

4.4 Clast Orientation Measurement

The spatial orientation of any clast can be described by the strike and dip of its plane of maximum projection (the AB plane) and the trend of its A axis. A Brunton compass is typically used to measure these orientations directly from the clast, as is done in the field. However, the use of a Brunton was not possible in this study for two reasons. The first was the narrow space in which to work, being confined by the 0.15m width of the deposition section. The second was the unreliability of the compass, due to the abundance of steel in the area around the depositon section.

Instead, a clast orientation simulator was constructed (Fig. 4-1). The simulator consisted of a 0.10 m x 0.15 m clear acrylic plastic plate, 6.4 mm thick, attached to a 0.30 m square plywood base by a flexible, semirigid plastic stem 0.15 m long. This device rested on a platform, temporarily attached to the front of the deposition section, at the same level as the deposit inside the section (Fig. 4-2). The plastic plate could be

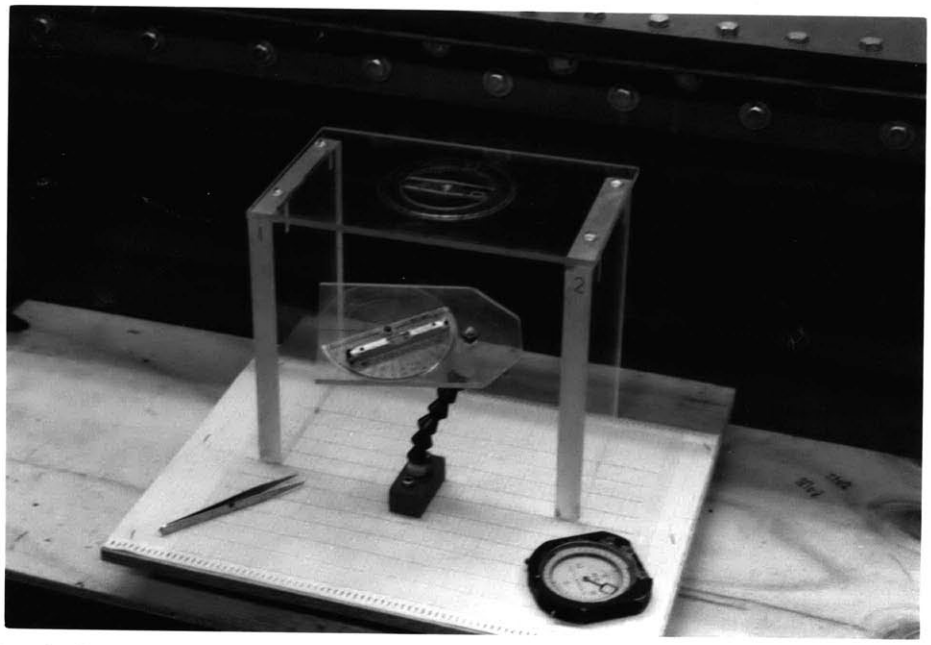

Figure 4-1: Clast Orientation Simulator

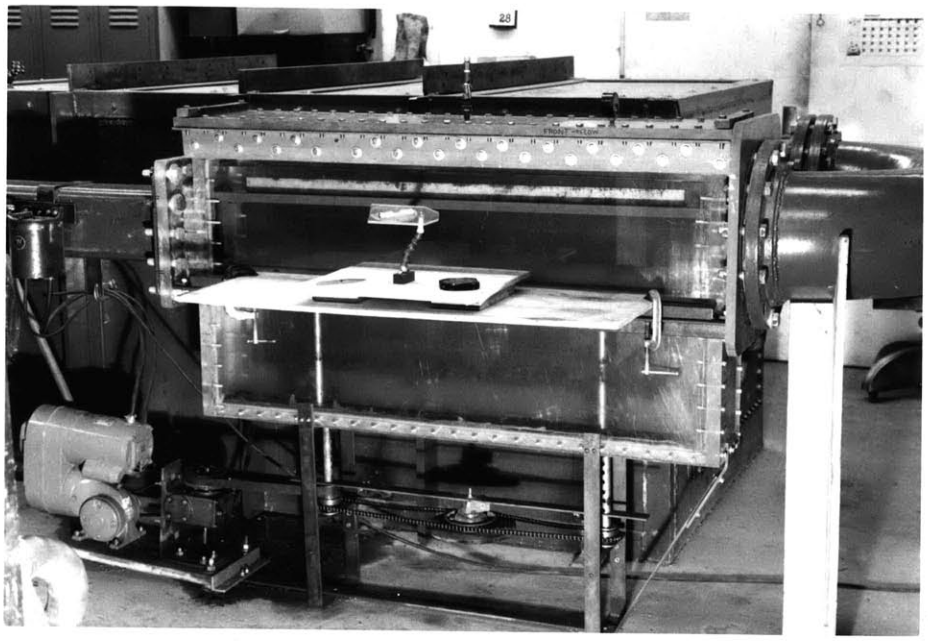

Figure 4-2: Set-up of Simulator For Orientation Measurements

twisted about into an orientation similar to that of a clast inside the section, and the orientation measurements taken from the plate.

The face of the plate represented the AB plane of the clast, and a single black line drawn lengthwise along the centerline of this face represented the A axis. A semicircular, clear plastic protractor was mounted on this face by a single screw through the origin of the protractor and the black line. A spirit level was fixed to the protractor, aligned parallel to its baseline, and could be leveled by rotating the protractor.

To measure the orientation of a clast, the plate was twisted about until the plate was parallel to the AB plane of the clast and the black centerline was parallel to the A axis. The protractor was rotated to level the spirit level, thereby making the baseline of the protractor horizontal. This baseline represents the strike of the AB plane. Arbitrarily defining the direction of flow as due north, the trend of the A axis and the strike of the AB plane were recorded as x degrees east or west of north. These trends were measured by positioning a 360 deg protractor, mounted horizontally on a clear acrylic stand, vertically above the plate, and measuring the angle between the flow direction and either the vertical projection of the A axis or the strike of the AB plane.

The two other orientation measurements taken were the

rake of the A axis in the AB plane, given by the angle between the strike of the AB plane and the A axis, and the dip of the AB plane, measured with an inclinometer held gently against the plate, perpendicular to the strike.

Several calculations were made to obtain the final orientation of the clast. The trend of the A axis was checked by the equation

$$\tan A = \cos D \tan R$$

where A is the angle between the trends the vertical projections of the A axis and the strike of the AB plane, D is the angle of dip of the AB plane, and R is the rake of the A axis in the AB plane. The angle A was either added to or subtracted from the measured strike of the AB plane to obtain the calculated trend of the A axis. The difference between the observed A-axis trend and the calculated A-axis trend was generally only one or two degrees. If the difference was greater than five degrees, the measurement was discarded. A second calculation was made to obtain the plunge of the A axis. The equation used was

$$\sin P = \sin D \sin R$$

where P is the angle between the A axis and the horizontal, and D and R are the dip of the AB plane and the rake of the A axis in the AB plane, respectively. The

direction of the plunge was south if the A axis dipped upstream and north if it dipped downstream.

To summarize the orientation measurement procedure: the plate was manually positioned to have an orientation similar to that of the clast to be measured; the semicircular protractor was rotated to find the strike of the AB plane; the trends of the A axis and the strike of the AB plane were measured; and the angles of the dip of the AB plane and of the rake of the A axis in the AB plane were recorded, and used to calculate the plunge of the A axis and to check the accuracy of the observed A-axis trend.

The deposition section was drained prior to orientation measurement, and the inner floor was slowly raised to bring the deposit into a more accessible position. A clast was selected for measurement according to the following criteria:

(i) it had a readily definable AB plane and, if possible, A axis;

(ii) it was rounded or well rounded;

(iii) it had a minimum A-axis length of about 15 mm;

(iv) it was deposited at least 25 mm from the sidewalls and 0.1 m from the endwalls;

(v) it was not in the lower 80 mm or the upper 30 mm of the deposit.

Finer sediment was gently blown away from around a

clast to be measured using an air hose, to reveal as much of the shape of the clast as possible, and the orientation was measured. If there was no obvious A axis, the strike and the dip of the AB plane were taken alone. When the orientation was measured, the clast was carefully removed and numbered, and the lengths of the principal axes were measured to the nearest millimeter by the method described earlier. All the clasts from a particular run were stored together to be referred to, if necessary, at a later time.

During the dissection process, notes were made describing any notable features of the deposit, and photographs of the deposit were taken from various directions upon completion of the orientation measurements. All the sediment from the deposit was dried and a grain-size analysis of the deposit made, including the weights of the stored clasts in the final distribution calculation.

Chapter 5
Results

5.1 General

Six official runs were attempted. Four were a complete success, one (Run 1) was a partial success, and one (undesignated) was a failure. The first run (Run 1) was made using the original trial feed-sediment mix that was described earlier, resulting in a deposit containing an insufficient number of measurable clasts. Even though no quantitative data were obtained from the run, it provided valuable insight to the transport processes that could be expected with the system, as well as to the nature of the deposit relative to the sediment transported. Also, the procedures for sediment feed, control of the flow, and generation of the deposit process were tested simultaneously for the first time, with positive results, and minor operational changes were made before the next run. The conditions of the four runs from which clast orientation and other data were obtained are summarized in Table 5-I.

The unsuccessful run was a first attempt at making a deposit at the highest flow and feed rates used in these

Table 5-1: Run Conditions

Run	Water Discharge (m^3/s)	Mean Depth Range* (m)	Mean Flow Velocity Range (m/s)	Sediment Discharge (kg/s-m)	Deposition Rate (mm/s)
3	0.054	0.13-0.14	2.5-2.8	39.5	0.94
2	0.041	0.13-0.14	1.9-2.1	13.3	0.60
4	0.027	0.10-0.11	1.6-1.7	6.6	0.39
5	0.024	0.10-0.11	1.4-1.6	2.6	0.26

*The Mean Depth values are given as a range due to localized variations in the measured depths. This is reflected in the calculated Mean Flow Velocity values, which are also given as a range.

experiments, which were later successfully attained in Run 3. After about two-thirds of the total run time had elapsed during this unsuccessful run, it was discovered that the drive system had failed, resulting in a delta-like deposit of no use. The run was stopped and the necessary repairs made, with no serious damage to the drive system.

5.2 Run 2

The moderately high flow and feed conditions used in Run 2 resulted in the sediment being transported mainly by saltation and suspension, with tractional transport having a minor role in the movement of only the coarser size fractions. As might be expected, the smaller fractions (less than 10 mm) were carried in suspension by the flow at all heights above the bed, and were also the main constituent of the bed itself. The upper 1-2 mm of the bed consisted of mostly of the finer sizes and moved downstream in a shearing style. The larger clasts, however, moved downstream in saltation, spending up to several seconds in contact with the bed. While suspended in the flow, a clast was generally oriented with its long axis parallel to the flow direction and its maximum plane of projection subhorizontal, dipping slightly upstream. As it came in contact with the bed, the upstream end would drag along the bed surface. At this point the clast would

either be lifted back into suspension, or it would begin to plow along the bed while remaining in an orientation similar to its orientation while in suspension.

Although the exact reason why a given clast becomes permanantly deposited is not known with certainty, several mechanisms were observed. If a clast, while moving along the bed surface in the plowing mode, becomes overlain on its upstream-dipping face by another clast, which is also moving by plowing along, or has just come out of suspension, its downstream velocity is reduced. As several more clasts join into this shingle-like chain, it becomes more difficult for the leading clast to continue, until finally the entire group becomes fixed on the bed. The result is an imbricated pocket of large clasts surrounded by the finer-grained matrix. The second mechanism involves only a single clast. While moving along the bed surface this clast becomes slowed in the "soupy", shearing upper fine-grained layer. Its angle of imbrication steepens, and its edges become buried by additional finer sediment coming out of suspension, finally reducing its downstream movement to zero.

The deposit formed during Run 2 had a striking fabric defined by the orientation and situation of the coarse clasts in the fine matrix. The photos taken of the flow-parallel and flow-normal cross sections upon completion of the clast-orientation measurements show this

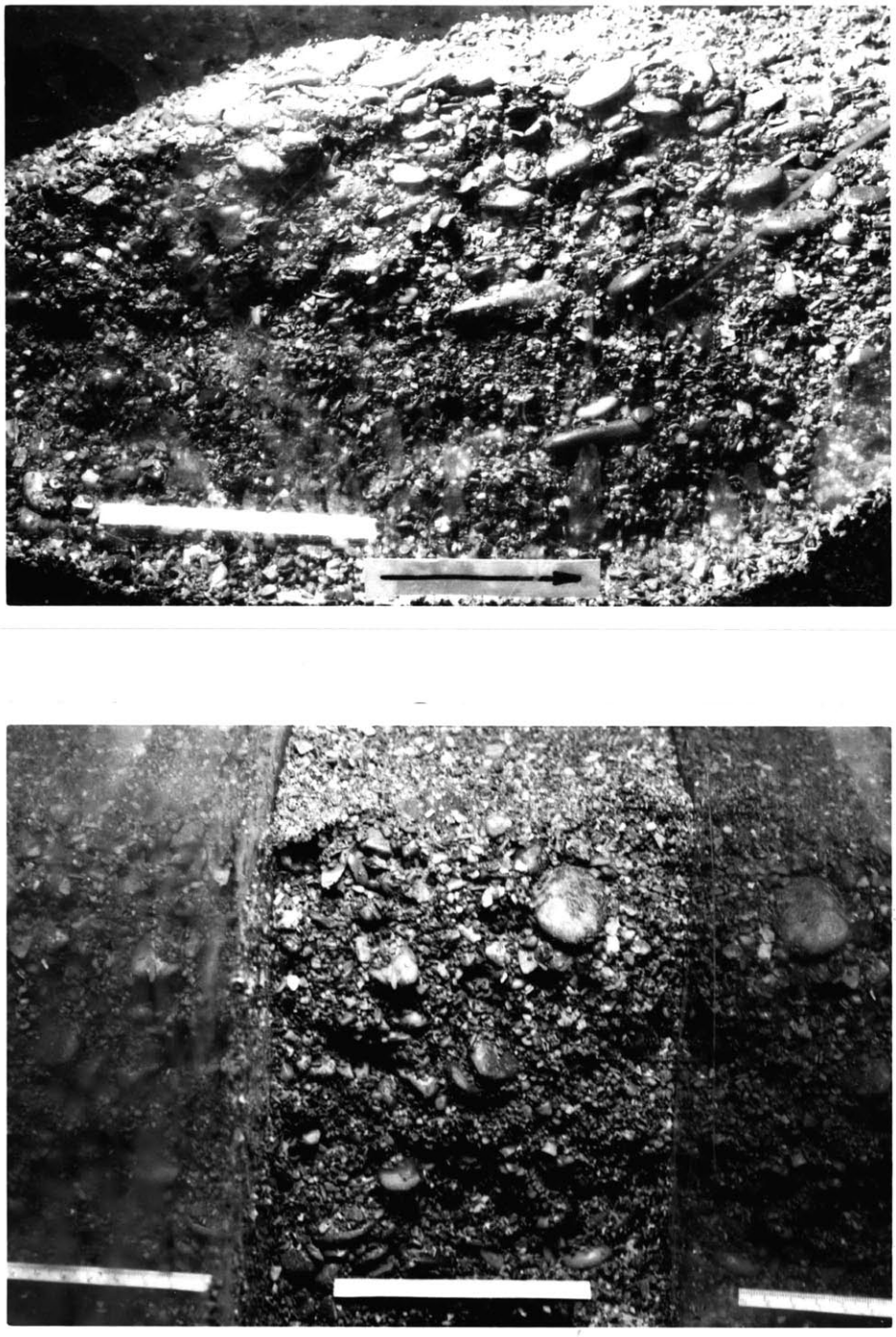

Figure 5-1: Deposit of Run 2: Flow-parallel and Flow-normal Cross-sectional Views

fabric quite well (Fig. 5-1). There is a definite upstream dip of the AB plane, and a flow-parallel trend to the A-axis orientations. Plotting the cumulative grain-size frequency curves (Fig. 5-2) allows a statistical description of the deposits. The median size of the deposit of Run 2 is only 3.48 mm (-1.8 phi) compared to a median size of 8.57 mm (-3.1 phi) for the sediment fed into the system, and therefore of the sediment in transport. The deposit also is negatively skewed (skewed towards the finer sizes), while the transported sediment is skewed towards the coarser sizes. In general, the deposit is markedly deficient in the coarser fractions, with only 25 percent of the clasts larger than 8 mm (sieve diameter).

From the deposit, 339 usable orientation measurements were obtained, 318 with both C axis and A axis data. The actual clasts measured are shown in Figure 5-3. The clasts ranged in maximum length from 13 mm to 63 mm, with a median size of 23 mm. The B/A and C/B axial ratios were calculated and each clast was placed in one of the four Zingg shape groups. The resulting shape distribution is shown in Figure 5-5. The rodlike clasts make up only 10 percent of the total sample, and only one clast was measured from the equant category. Equant clasts are generally underrepresented because of the lack of an obvious A axis direction and AB plane. Figure 5-7 shows

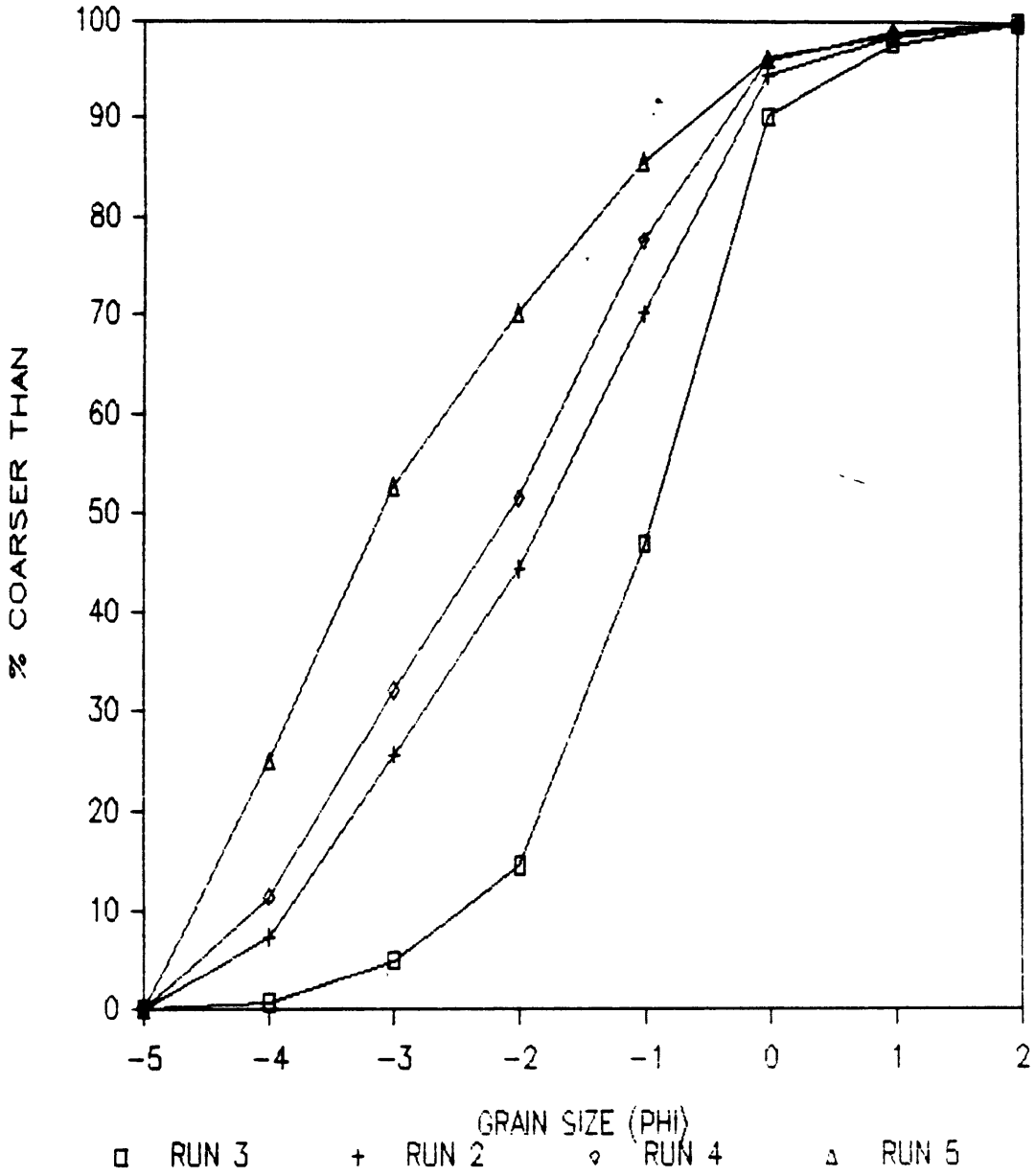

Figure 5-2: Cumulative Grain-Size Distribution Curves Of The Deposits Formed During The Official Runs

Figure 5-3: Clasts measured from Run 2

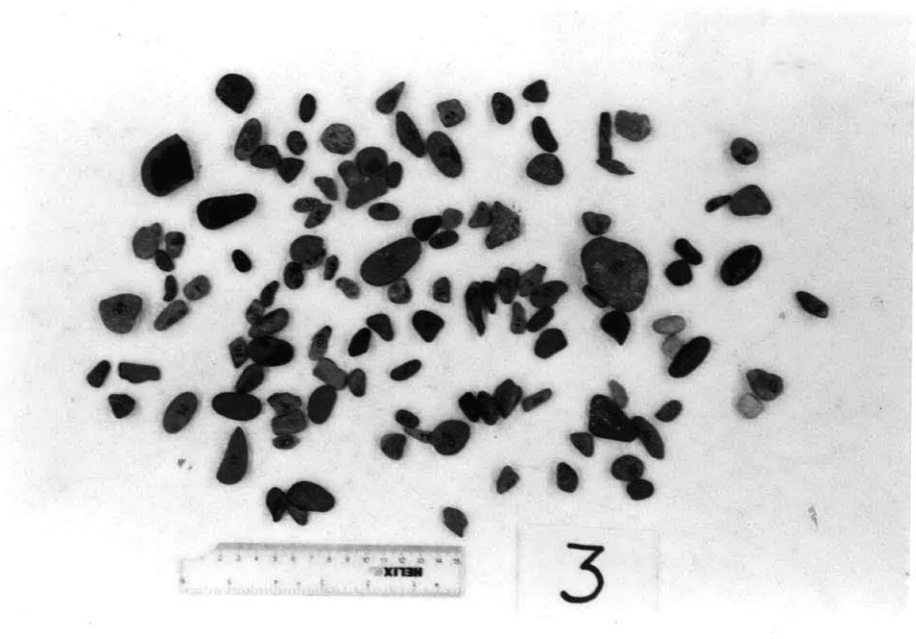

Figure 5-4: Clasts measured from Run 3

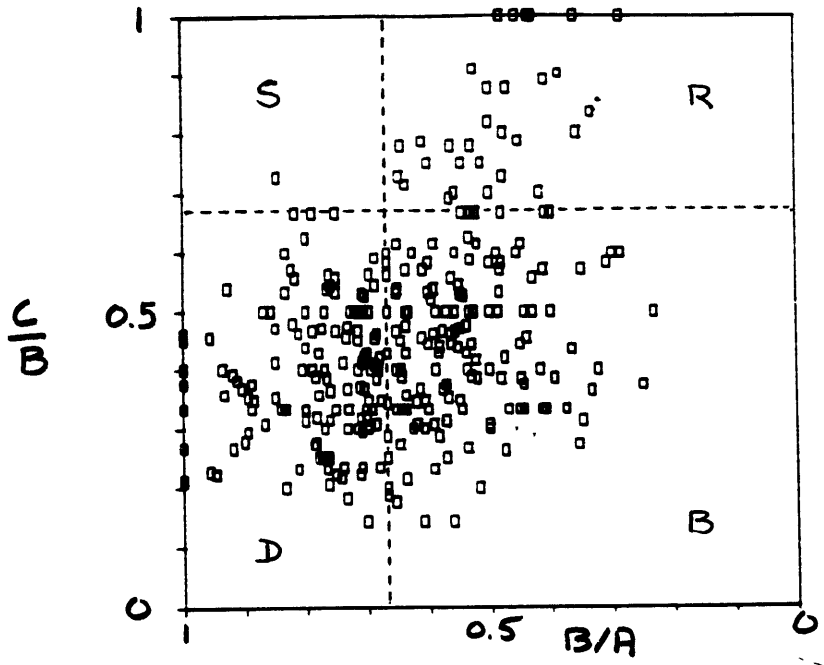

Figure 5-5: Zingg-Shape Distribution of the Measured Clasts of Run 2

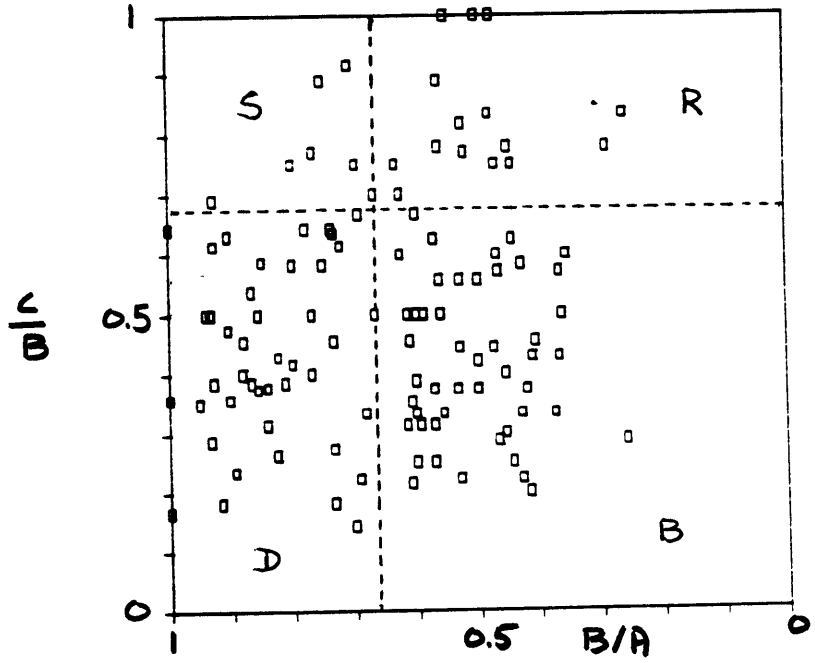

Figure 5-6: Zingg-Shape Distribution of the Measured Clasts of Run 3

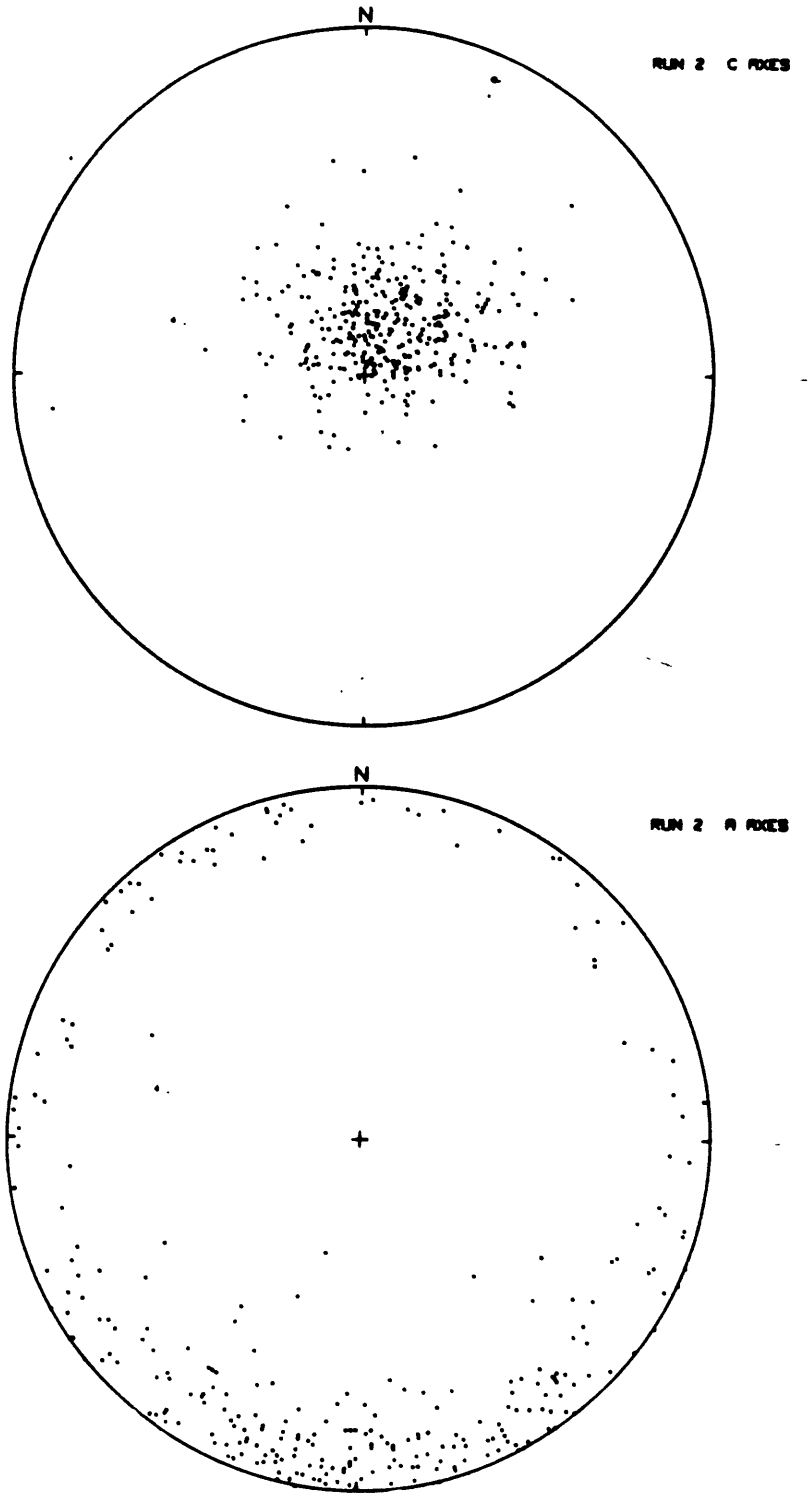

Figure 5-7: Schmidt-Net Plots of the C and A Axes of Run 2

equal-area Schmidt-net plots of the C axes and the A axes. The C axes show an obvious preferred orientation, generally trending in the direction of flow (north) with a very steep, and in some cases vertical, plunge. The A axes, however, show much more scatter, being oriented in all directions with plunges between 25 deg and horizontal. The angles between the trend of the A axis and the direction of flow (the deviation angle) were grouped into 10 deg intervals, and the frequency of the groups computed for the entire sample and for the three major shape groups- rods, disks, and blades (Fig. 5-8). The overall trend is a moderately strong flow-parallel orientation. The rod-shaped clasts show a very strong flow-parallel orientation, with 63 percent deviating 20 deg or less from the flow direction. The bladed clasts have a moderately preferred parallel trend, while the disks show a weakly preferred parallel trend.

5.3 Run 3

The flow conditions in Run 3 were the strongest of the four official runs. All size were transported in uniform suspension. The result was an opaque flow in which the orientation of the clasts could not be clearly seen through the sidewalls. The smaller clasts were dispersed at all heights above the bed, while the coarser clasts were transported mainly in the lower half of the

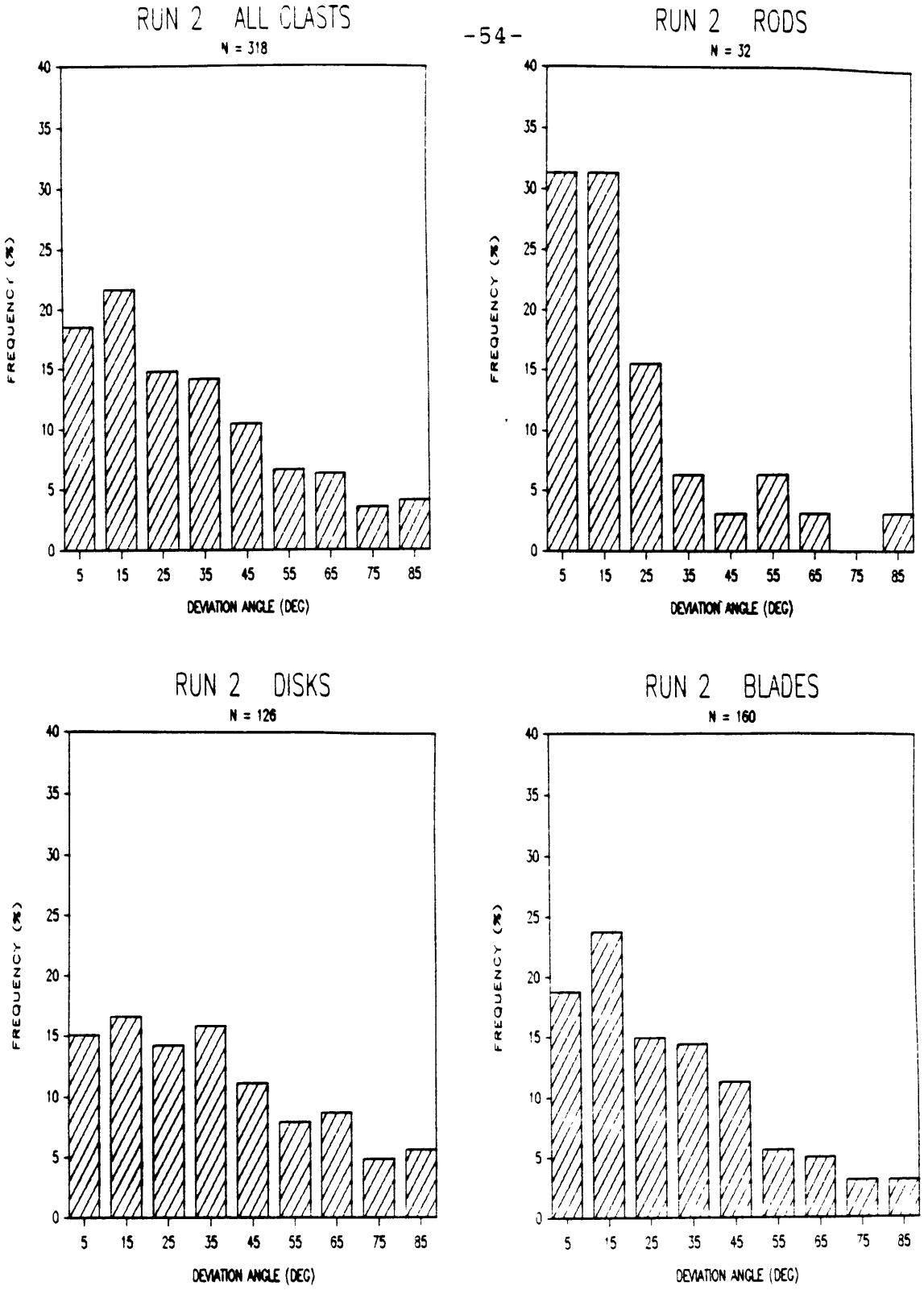

Figure 5-8: Deviation Angle Frequency Distribution of Clasts of Run 2 Grouped By Zingg Shape

flow. Occasionally a large clast would come into contact with the bed, but it immediately was taken back into suspension, allowing no time for it to become deposited as in Run 2. The deposit formed was composed almost entirely of the finer size fractions, with no striking fabric characteristics (Fig. 5-9). The cumulative size distribution (Fig. 5-10) shows that only 5 percent of the clasts deposited were in the 8-32 mm size fraction, the median size being only 1.93 mm. The very small proportion of large clasts that were deposited were scattered in isolation throughout the dominantly fine-grained bed.

Because of the small number of large clasts in the deposit, the orientation of only 118 clasts (105 with A-axis data) could be measured. To find if the sample was large enough to give accurate results, cumulative frequency curves of the deviation angle were plotted (Larsson, 1952) for the first 25 clasts, then the first 50, then the first 75, and finally all 105 (Fig. 5-10). Little variation is seen between the curves for 75 and 105 clasts, indicating that additional orientation measurements would not have altered the result significantly. (It is therefore justifiable that the sample sizes of the other three runs, in which more clasts were measured, are also sufficiently large, and this test was not repeated for those runs.) The sample of measured clasts (photographed in Figure 5-4) has a range of A axis lengths from 12 mm to

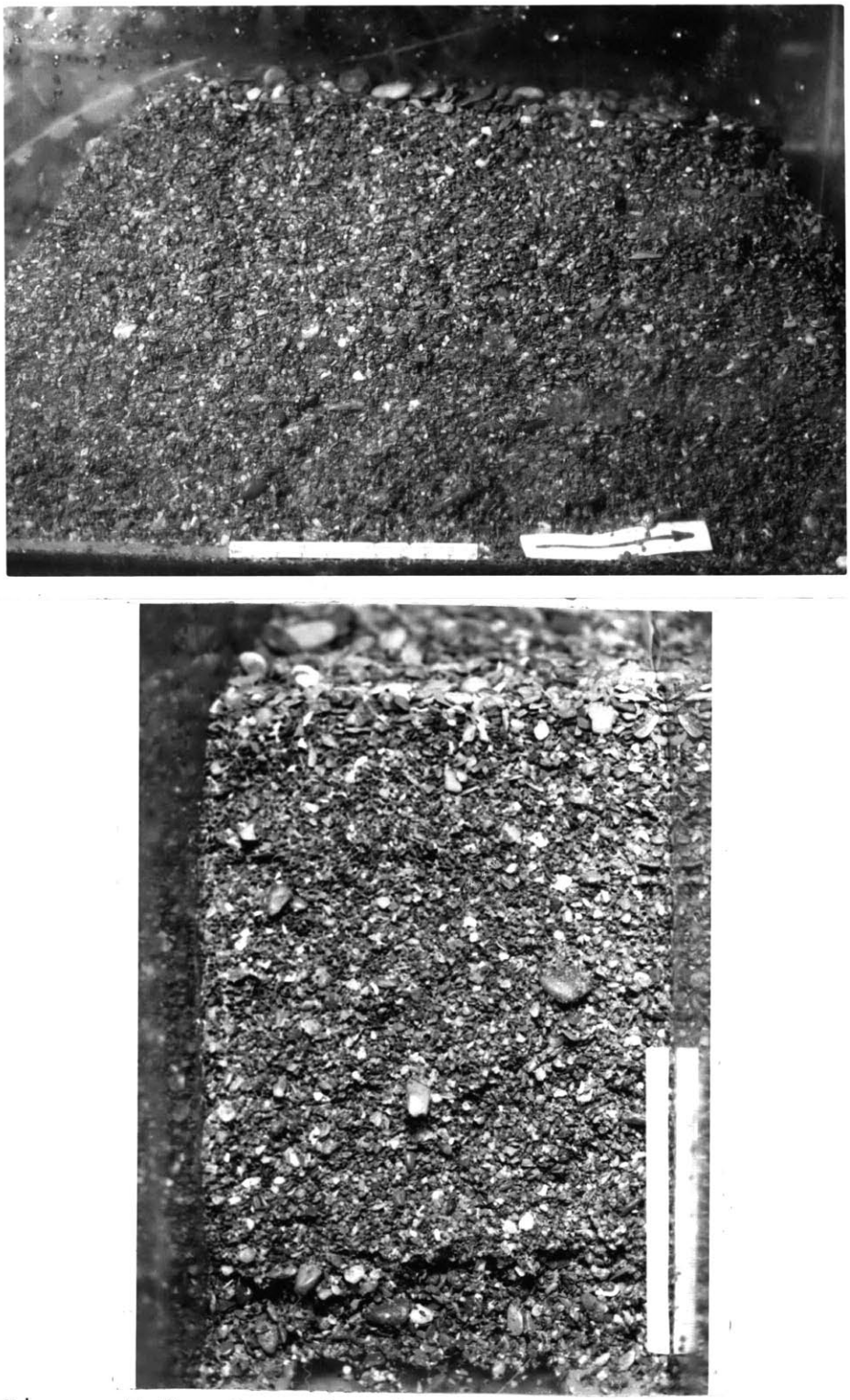

Figure 5-9: Deposit of Run 3: Flow-parallel and Flow-normal Cross-sectional Views

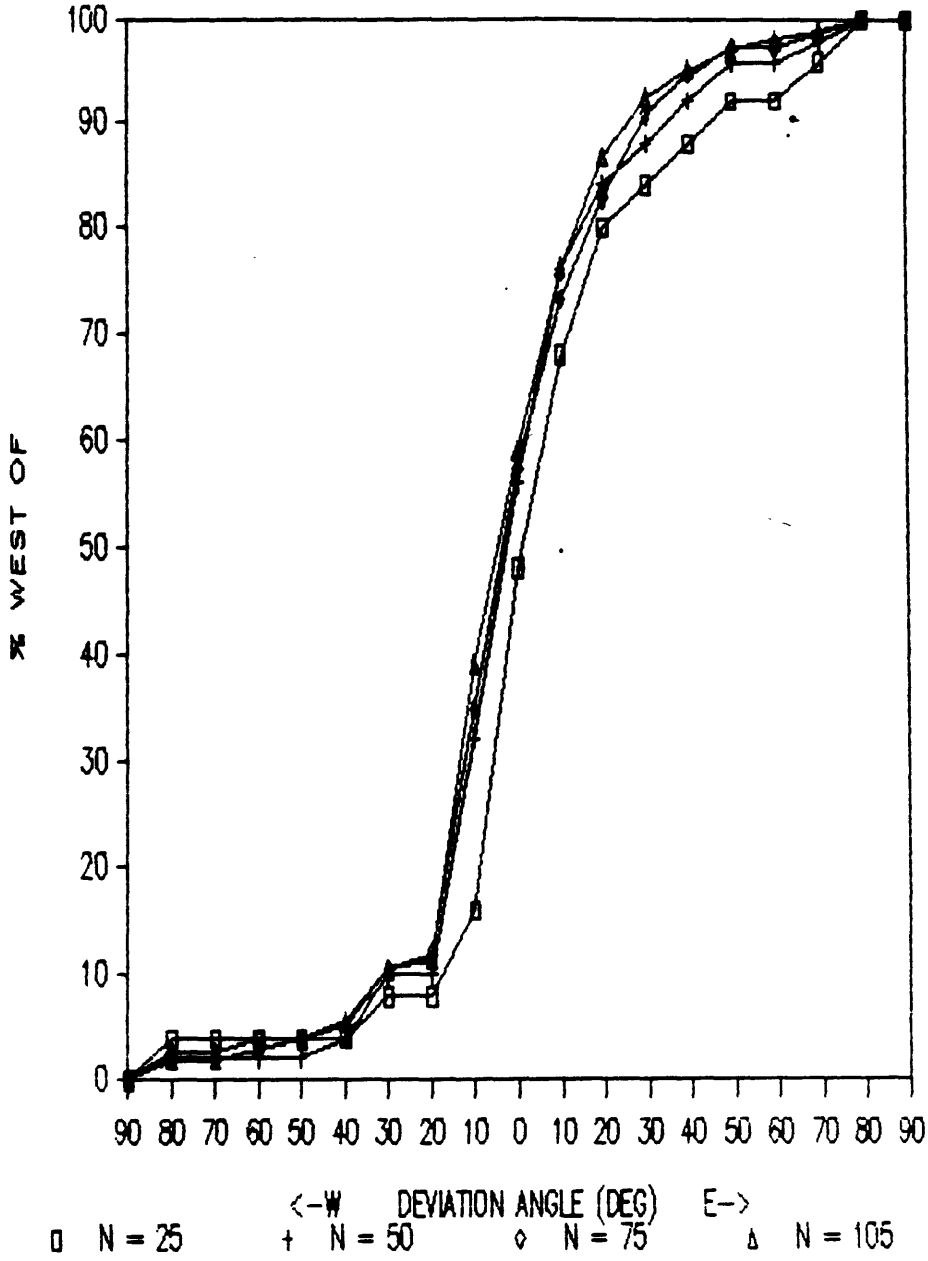

Figure 5-10: Cumulative Directional Diagram For Varying Numbers of Clasts of Run 3

44 mm, with a median size of only 18 mm. About 50 percent of the clasts were blades, 29 percent disks, and 16 percent rods. Figure 5-11 shows the stereonet plots of the C axes and the A axes. The C axes show a preferred orientation similar to Run 2, with a flow-parallel trend and dipping upstream. The A axes show a preference for a flow-parallel orientation also, with a shallow downstream dip. The A axes of Run 3 show much less scatter than in Run 2, but this may be only apparent rather than real, because of the smaller number of points. The frequency histogram of the deviation angle (Fig. 5-12) reveals that the orientation is actually much better defined than in Run 2, with almost 62 percent of all the clasts measured aligned within 20 deg of the flow direction. Even more striking is the preference of the rod-shaped clasts to be aligned parallel to flow: almost 60 percent are within 10 deg of the flow direction, and 77 percent are within 20 deg. The disk-shaped and blade-shaped clasts also show a strong flow-parallel orientation, although not as strong as that shown by the rods. It is conceded that the populations of these shape groups are small, but the anisotropy of orientation seems too well defined to be accidental.

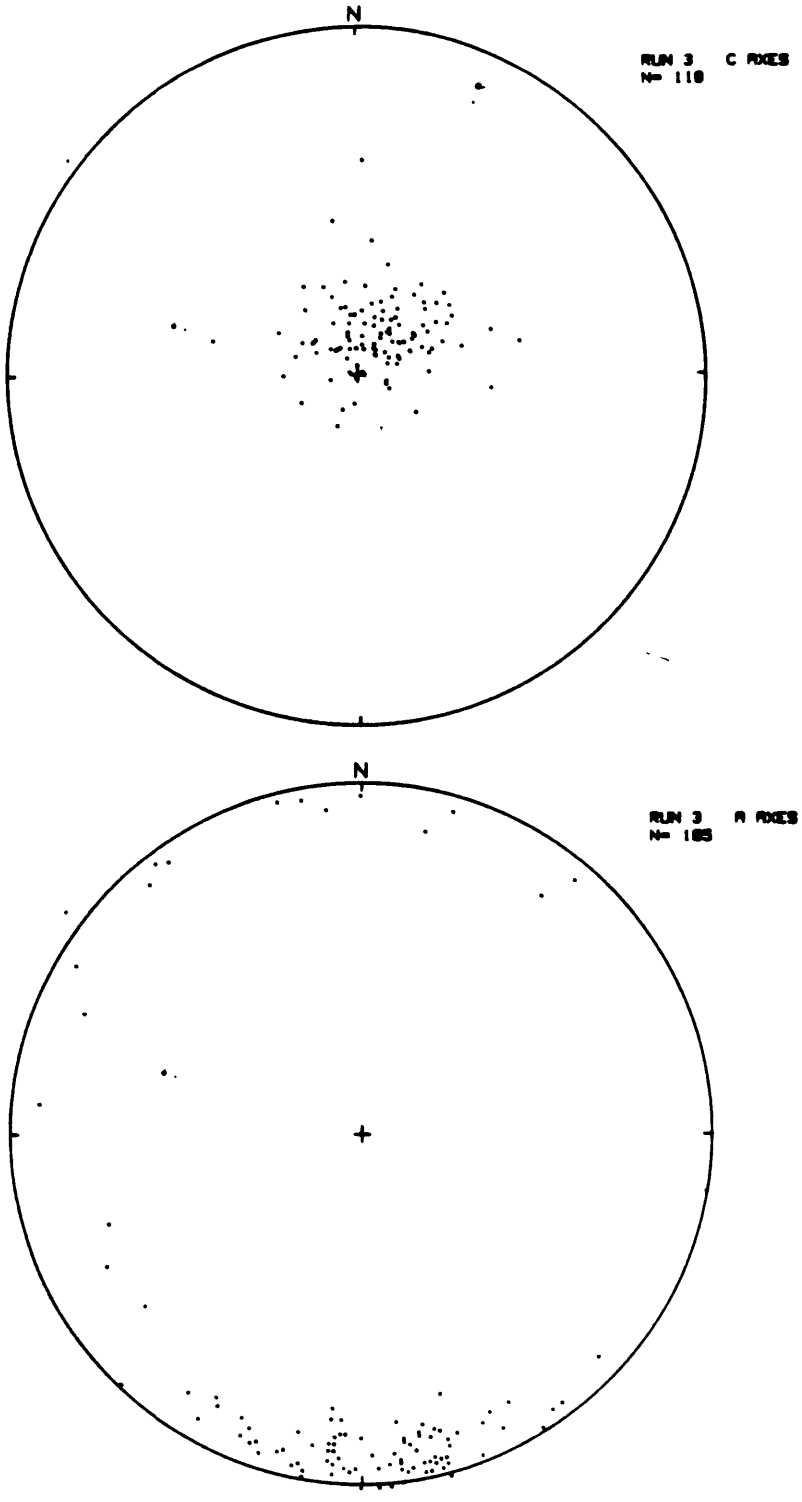

Figure 5-11: Schmidt-Net Plots of the C and A Axes of Run 3

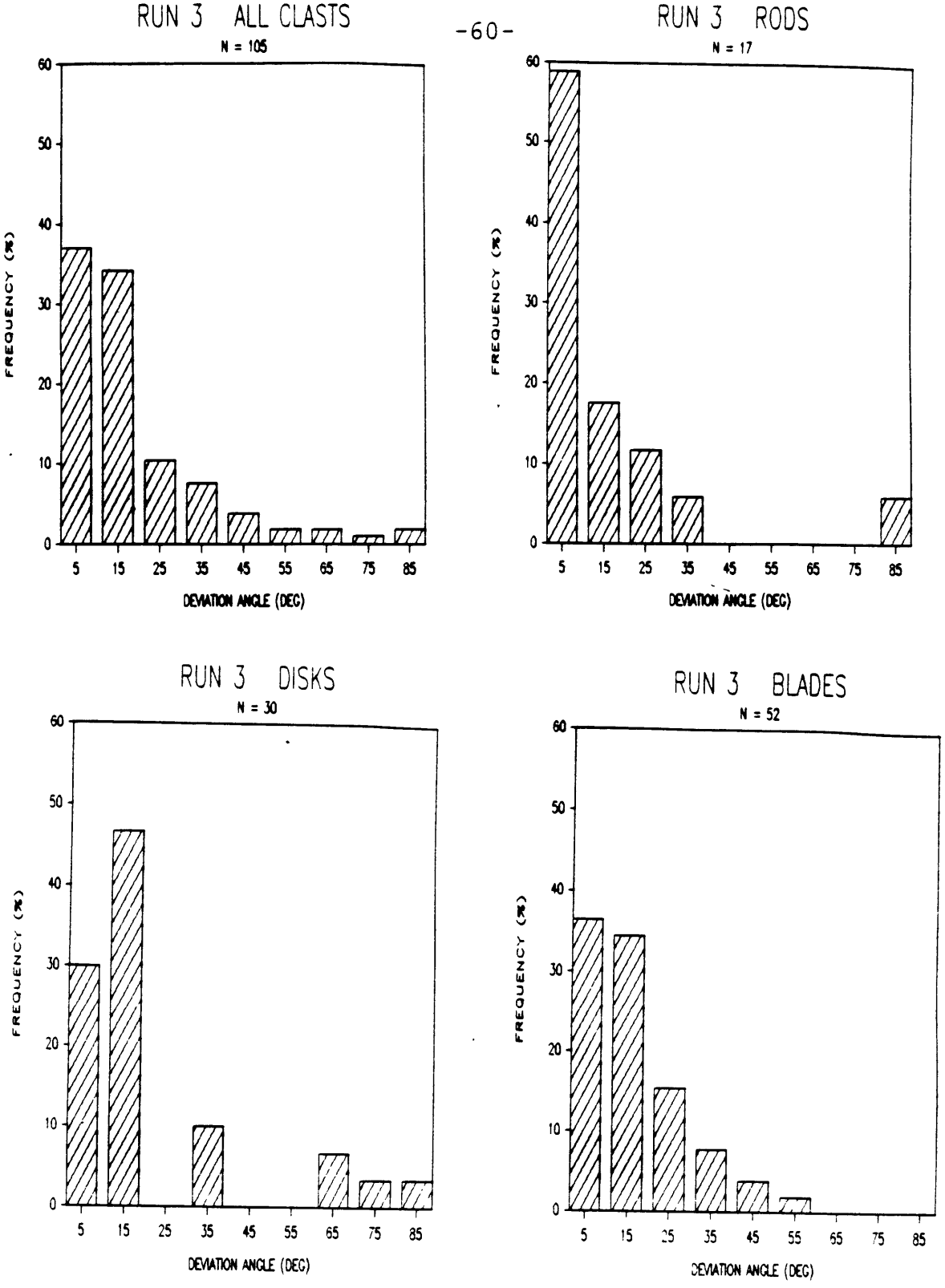

Figure 5-12: Deviation Angle Frequency Distribution of Clasts of Run 3 Grouped By Zingg Shape

5.4 Run 4

The flow conditions in Run 4 were much less strong than in Runs 2 and 3. The feed rate was one-third of that of Run 2, and only one-sixth of that of Run 3. The result was a significantly different style of transport and deposition. Instead of all the sediment, regardless of size, being transported by suspension and saltation only, tractional transport was an important mechanism with the larger clast sizes. These larger clasts moved downstream mostly in a sliding or plowing fashion, as seen to a small degree in Run 2. The sliding clasts were oriented on the bed surface with their long axes predominantly parallel to flow and dipping upstream, although there was some rotational movement away from the flow direction as moving clasts collided with other clasts on the bed. Chains of imbricated clasts described in Run 2 were common, forming much more extensive units several clasts wide and deep. The smaller size fractions moved in and out of suspension, still forming most of the bed surface. Because of the lower flow velocity, the downstream movement of the clasts was much more readily halted by burial by the finer sizes.

The fabric of the deposit is well defined by the clasts (Fig. 5-13). The pockets of coarse clasts formed by the moving chains are preserved, with the interstitial spaces filled by the finer sediment. The cumulative size

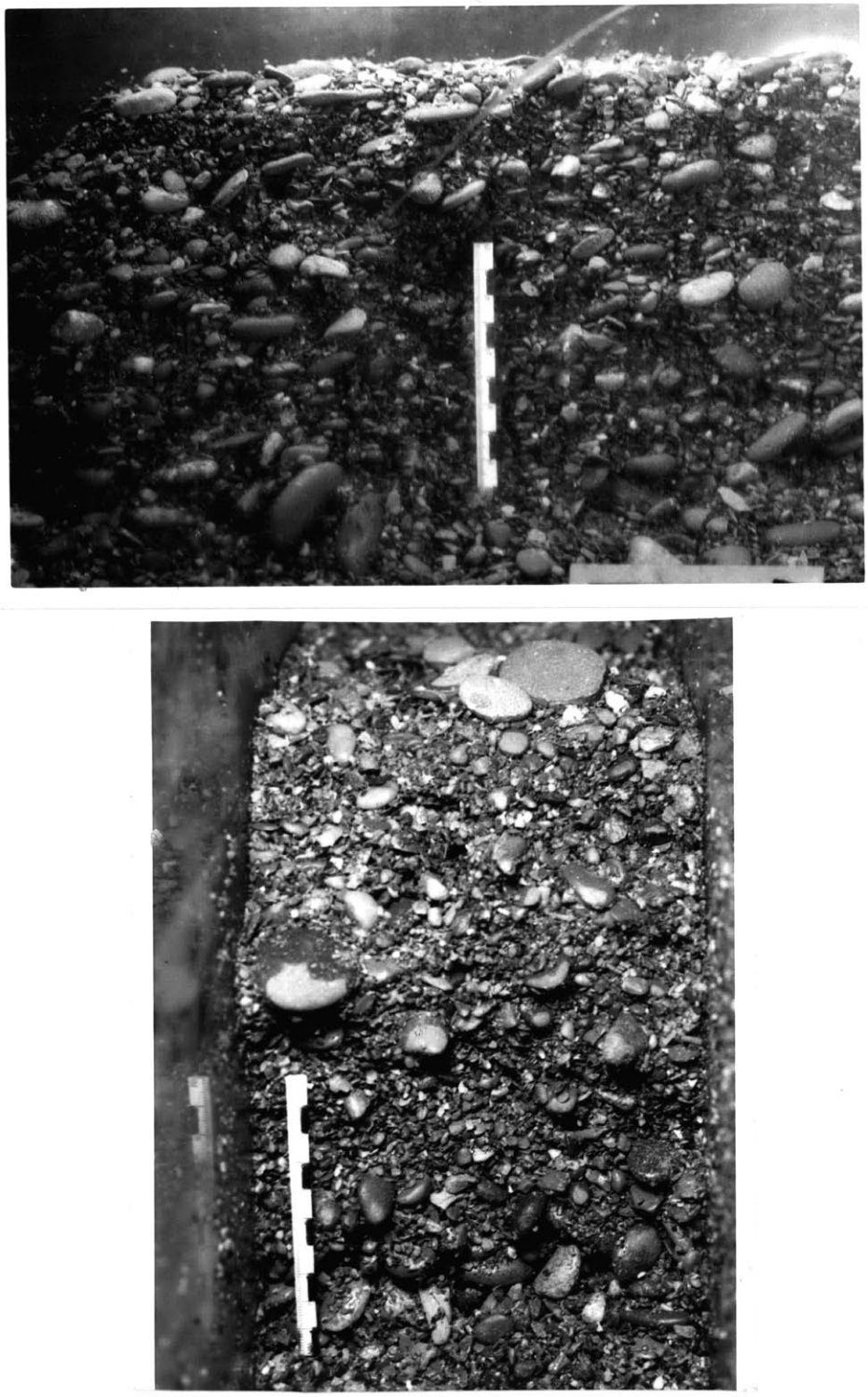

Figure 5-13: Deposit of Run 4: Flow-parallel and Flow-normal Cross-sectional Views

distribution (Fig. 5-2) close to being a normal ditribution (skewness value very near zero) and a median size of -2.10 phi (4.3 mm), which is very near the middle of the -5 phi to 1 phi range of the deposit.

Unlike the deposit in Run 3, that in Run 4 provided more than enough measurable clasts, with over 30 percent of the deposit having a sieve size greater than 8 mm. The orientations of 313 clasts (Fig. 5-14) were obtained, 302 of these having A axis orientation data. The maximum lengths of the sampled clasts range from 13 mm to 61 mm, with a median size of 21 mm. 30 percent of the clasts were disk-shaped, almost 60 percent were blade-shaped, and 10 percent were rod-shaped (Fig.5-16). The C and A axes are plotted in Figure 5-18. Once again, the C axes show a flow-parallel orientation, plunging steeply (70-90 deg) downstream, indicating a gentle upstream dip of the AB plane. The A axes, however, show much more scatter, somewhat similar to the A axes in Run 2.

The frequency histograms of the deviation angle for the entire sample and for each shape group are shown in Figure 5-19. The overall sample shows a moderately preferred flow-parallel orientation, with about 63 percent of the A axes exhibiting this preference. The rod-shaped clasts seem to have a bimodal frequency distribution with both parallel and oblique modes. The disks show a weak flow-parallel preference, while the blades have regular,

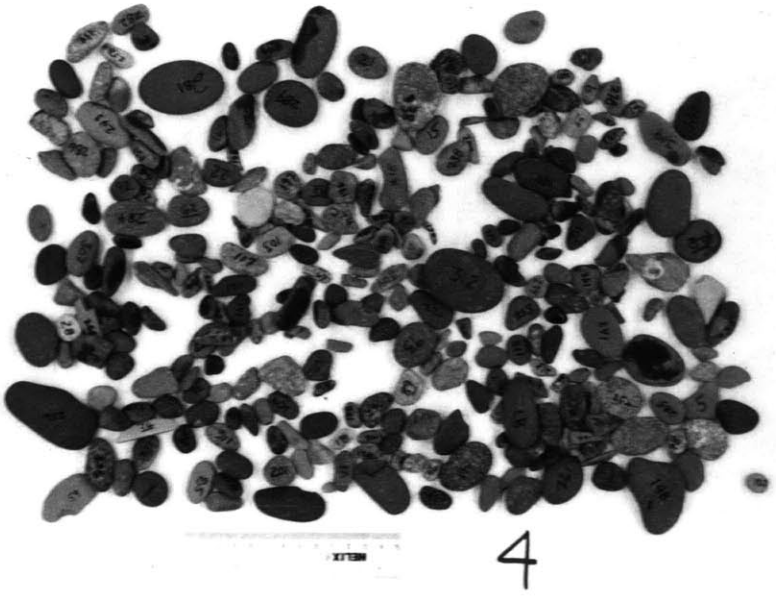

Figure 5-14: Clasts Measured From Run 4

Figure 5-15: Clasts Measured From Run 5

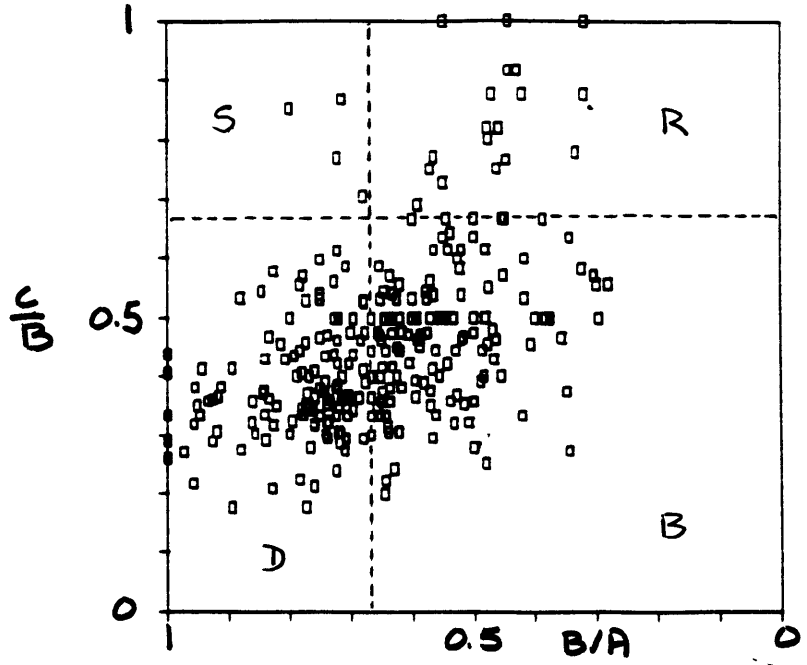

Figure 5-16: Zingg-shape Distribution of Measured Clasts From Run 4

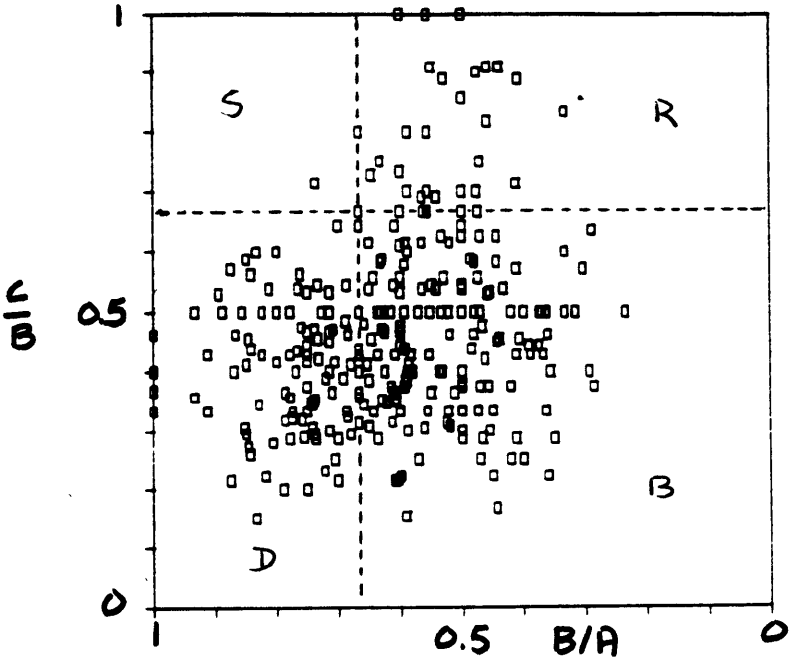

Figure 5-17: Zingg-shape Distribution of Measured Clasts From Run 5

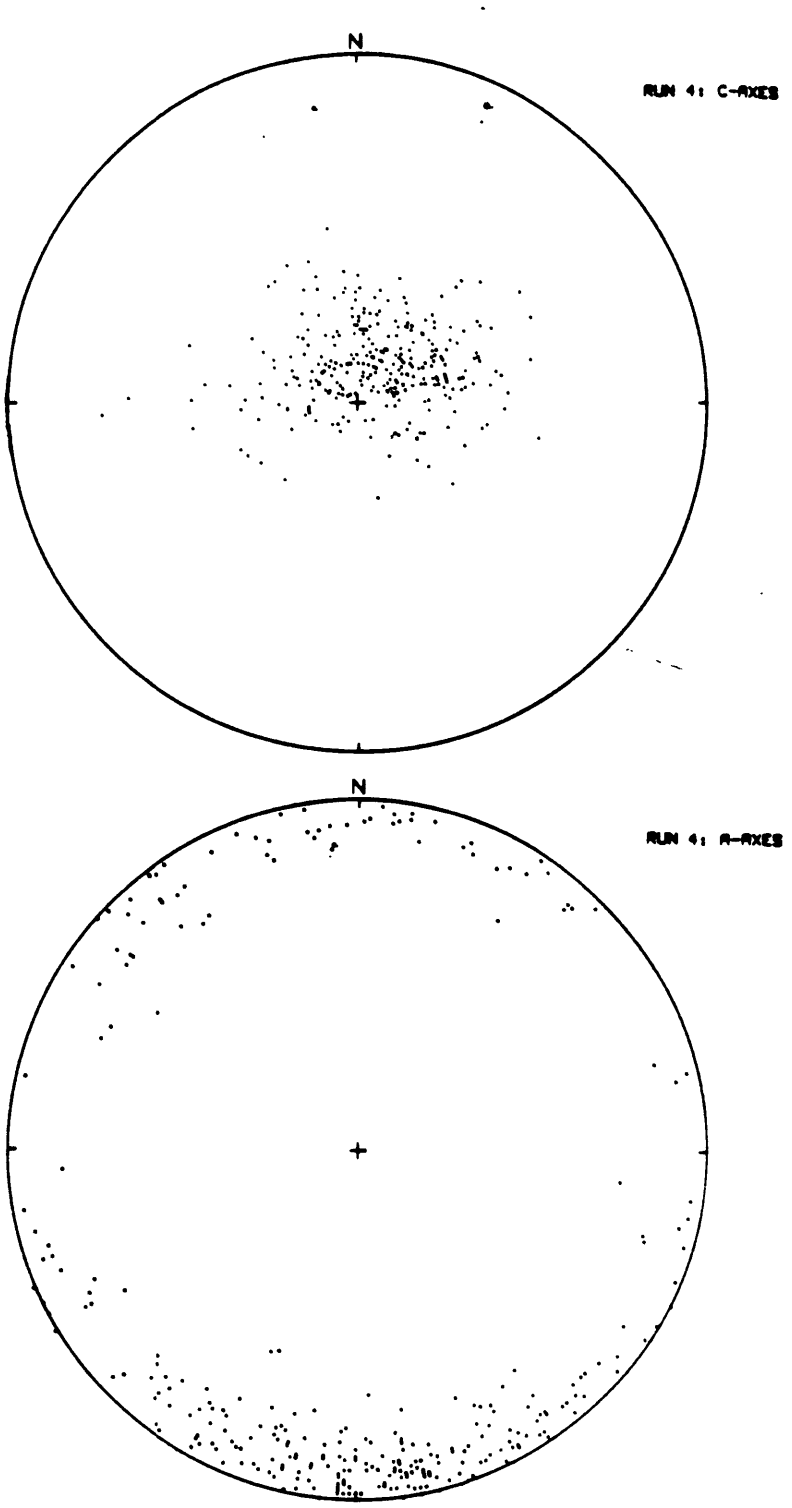

Figure 5-18: Schmidt-Net Plots of the C and A Axes of Run 4

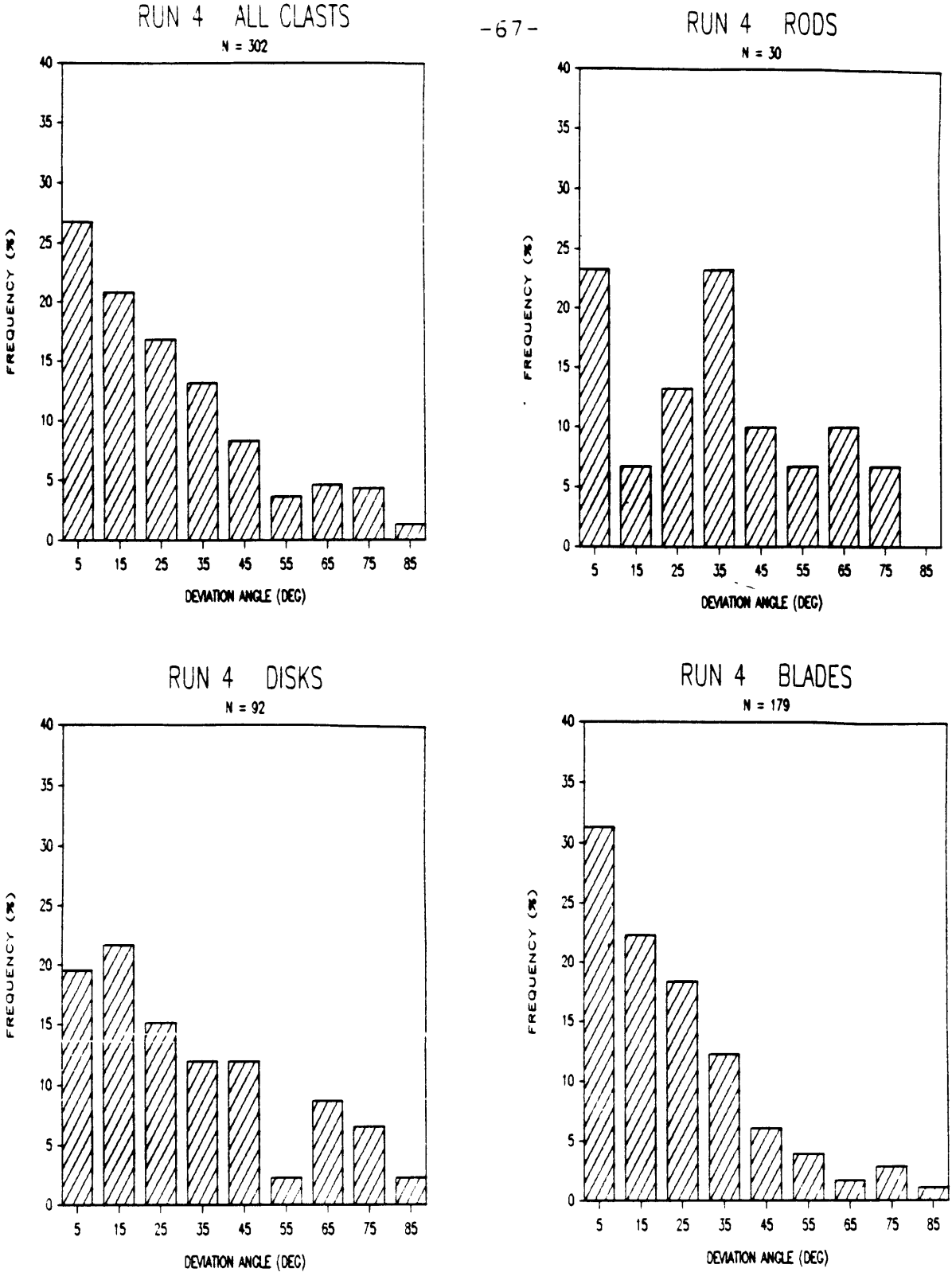

Figure 5-19: Deviation Angle Frequency Distributions of Clasts From Run 4 Grouped By Zingg Shape

nearly symmetrical distribution, with a flow-parallel maximum and flow-transverse tails.

5.5 Run 5

The lowest flow and feed rates were used in Run 5. The feed rate was only 6 percent of that of highest rate, used in Run 3. The result was transport of almost all of the sediment in traction or saltation. As in Run 4, the larger clasts slid downstream on the bed with a seemingly flow-parallel orientation. Many of large disk-shaped clasts rolled swiftly downstream like wheels. Generally, there was much more contact between the large clasts during transport and deposition than in the other runs. The finer sizes were transported mostly in saltation, with some carried in suspension. All the sediment moved downstream in the lower half of the flow. The resulting deposit is shown in Figure 5-20.

Originally thought to be pulsing caused by irregular feeding, passage of repetitive, distinctive bed forms or transport waves was observed during the run. After several seconds of low transport from the upstream section of duct, a distinct wave of coarse sediment came into view in the deposition section. The height of this wave was of the order of 1 to 2 cm. Although not measured at the time, it was estimated at moving downstream at about 10 - 15 cm/s. As the coarse wavefront moved steadily

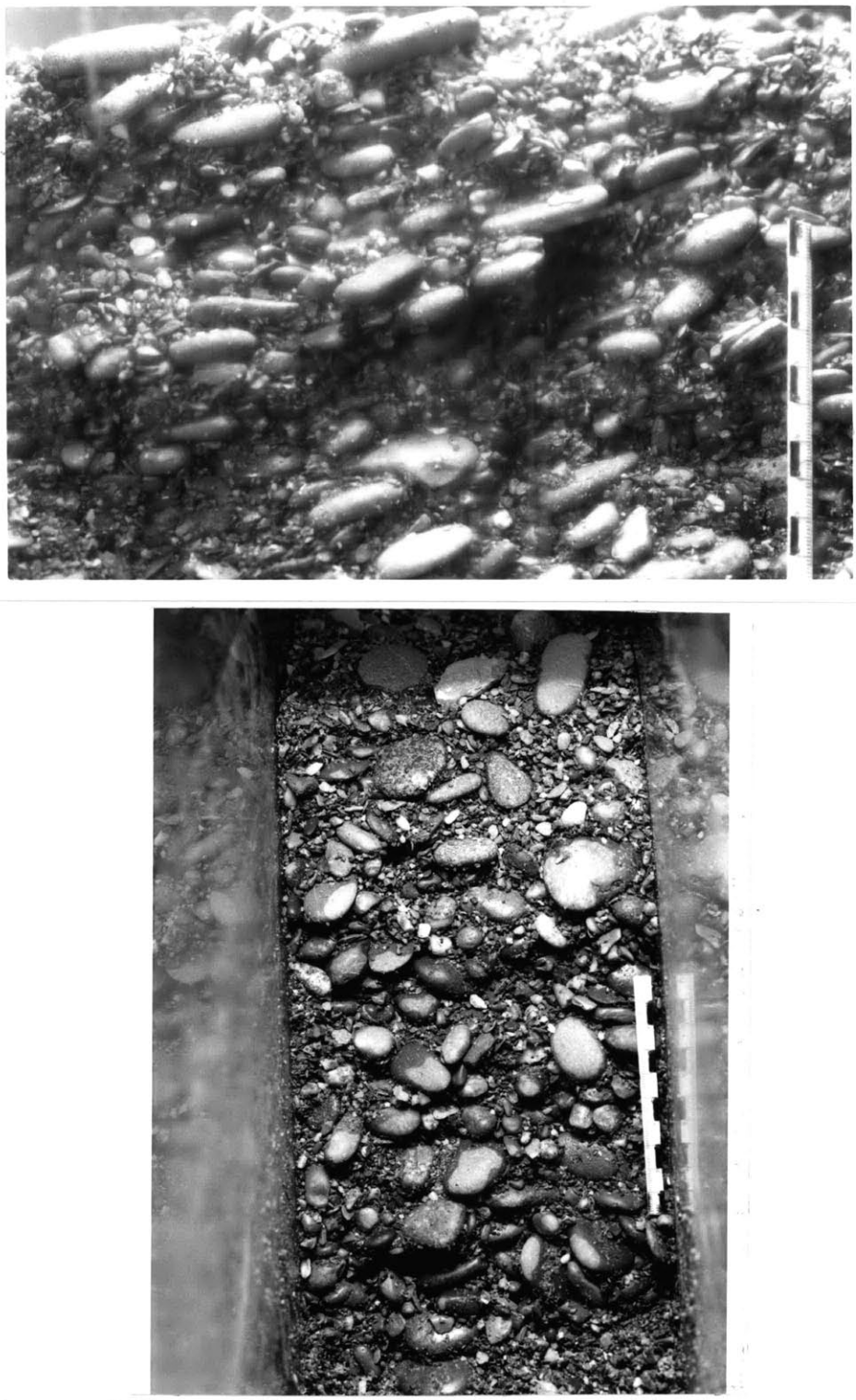

Figure 5-20: Deposit of Run 5: Flow-parallel and Flow-normal Cross-sectional Views

downstream, the sediment that trailed behind became increasingly finer in size and the transport rate gradually decreased, until the transport was reduced to a rate similar to that which preceded the coarse front. After several seconds another wave appeared from the upstream duct, again heralded by the sudden transport of the coarse clasts. The time between the appearances was timed, and was quite regular at 110 to 120 seconds. This wavelike structure formed an interesting fabric structure (Fig. 5-21). Lenses of openwork gravel were formed by the burial of the coarse wavefront, the interstitial spaces not being filled by finer sediment. When the deposit was dissected, the spaces were indeed found to be empty. The clasts were well imbricated, being arranged in the shingle-like manner described earlier.

Analysis of the grain-size distribution of the deposit produced a cumulative frequency curve that is almost identical to the curve for the original sediment mix (Fig. 5-2). In contrast to the deposits of Runs 2 and 3, the size distribution in Run 5 was positively skewed towards the larger grain sizes and had a median size of 8.57 mm. Fifty-two percent of the clasts had a sieve diameter greater than 8 mm.

Orientation data were collected from a sample of 299 clasts, shown in Figure 5-15. Of these, 272 A-axis orientations were measured. The maximum lengths of the

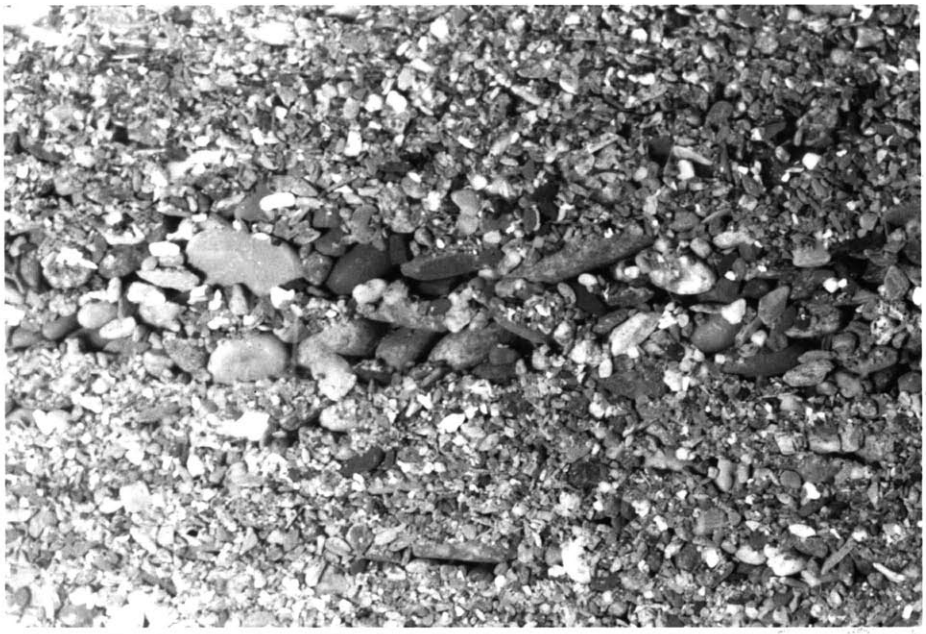

Figure 5-21: Openwork Gravel Lenses Formed During Run 5

clasts ranged from 16 mm to 57 mm with a median length of 27 mm. Thirty-eight percent were disk-shaped and 54 percent were bladed, while less than 7 percent were rod-shaped (Fig. 5-17). Plots of C-axis and A-axis orientation are shown in Figure 5-22. The C axes show more scatter than in the other three runs, but the general orientation is the same. The A axes, however, are distributed almost uniformly around the entire perimeter of the plot. The histograms of the deviation-angle frequencies are shown in Figure 5-23. The sample as a whole shows only a very weak parallel trend. The disk-shaped clasts show an almost uniform frquency distribution of the deviation angle from 0 deg to 90 deg. Both the rod-shaped clasts and the disk-shaped clasts appear to have bimodal distributions, with both flow-parallel and flow-transverse modes.

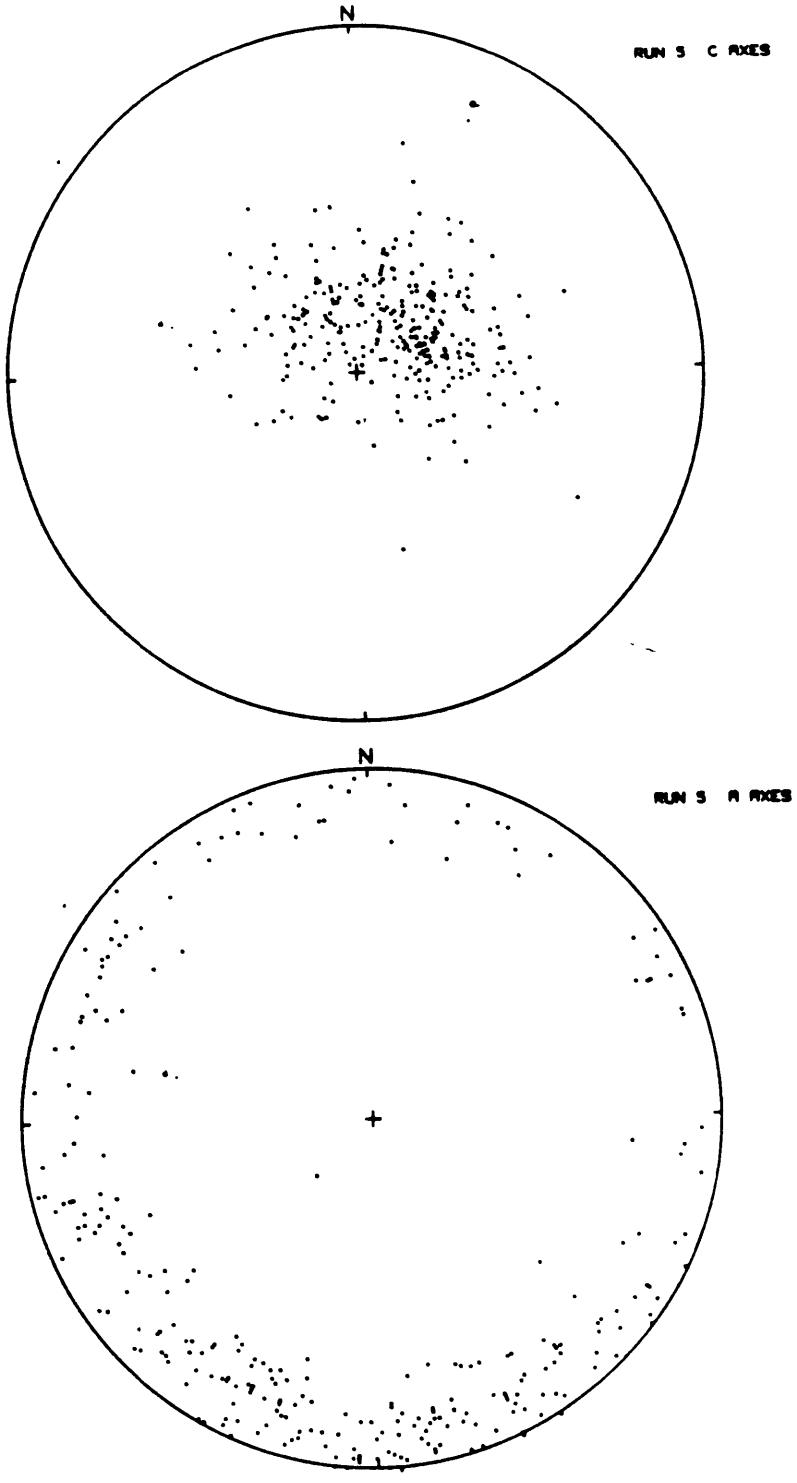

Figure 5-22: Schmidt-Net
Plots of the C and A Axes of Run 5

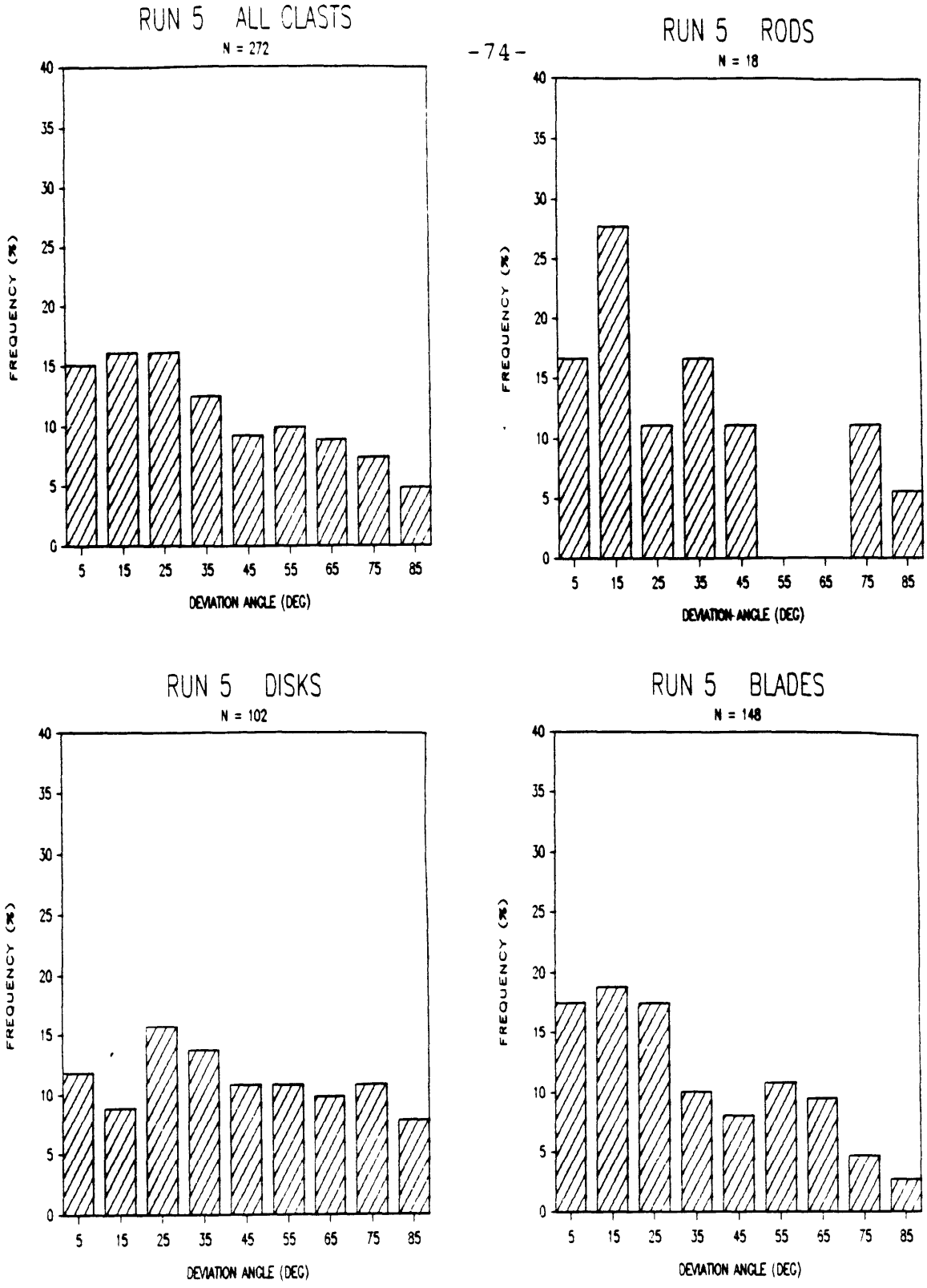

Figure 5-23: Deviation Angle Frequency Distribution of Clasts of Run 5 Grouped by Zingg Shape

Chapter 6
Discussion and Conclusions

From the results of the series of experiments described in the previous chapter, some definite conclusions can be drawn regarding the nature of deposits of high-velocity gravel-transporting flows. From the grain-size analyses of the deposits, a definite trend is observed. Figure 5-2 shows a steady shift in the size-distribution curves of the deposits. The higher-discharge flows are skewed toward the finer size fractions, with a negative skew value. Decreasing the flow skews the curve towards the larger size fractions, resulting in a positive skew value. The mean grain size was 8.57 mm for the highest-discharge run, while the mean grain size was only 1.93 mm for the lowest-discharge run.

It is commonly expected that the percentage of fine sediment in a bed is reduced by winnowing as the flow strength increases, resulting in an increasingly coarse deposit (Harms, 1975). In the present experiments, however, just the opposite is seen. This is probably because, with increasing flow strength, the time spent in contact with the bed by the larger clasts decreases, as they increasingly become transported by suspension instead

of by traction. This would decrese the possibility of deposition by burial or cessation of downstream movement. However, this does not explain why the finer material is deposited.

While in suspension, finer sediment tends to travel closer to the bed than the coarser sizes. Bagnold (1954) attributed this to dispersive-pressure effects. This dispersive pressure, created by clast collisions in grain flows, is greater on larger clasts than on smaller, because of the larger surface area. In response to this, larger clasts tend to move upward in the flow, to zones of lower shear stress, thus producing an upwardly increasing size gradation in the flow. Middleton (1970) proposed a different theory, that the upwardly coarsening gradation is created by a "kinetic sieve" mechanism, in which the smaller clasts, by mechanical means, tend to fall towards the bed between the larger clasts. Sallenger (1979) used Bagnold's theory to explain inverse grading within a deposit.

Walker (1975) discussed the common occurrence of inverse-to-normal grading in resedimented conglomerates. He mentions that it is not clear whether the shift from inverse grading to normal grading is produced by a single depositional process, or if the normally graded section was deposited unconformably on the coarser bed. The results of the grain-size analyses from these experiments

suggest that this inverse-to-normal grading might be the result of continuous deposition from a temporally decreasing flow that was originally strong enough to transport the coarser size fractions by suspension.

The main thrust of this research, however, was not to explore the mechanisms that control grading, but rather to analyze clast orientation under controlled laboratory conditions. The results are clear and consistent, but interpretation is necessary to make them useful. They can be looked at in two parts, which together provide interesting conclusions.

The data collected from the measurements of the orientation of the AB plane are fairly straightforward. The AB planes, represented by the poles of the planes (the C axes) show little variation in mean orientation from run to run, although the scatter increases slightly in the lower-discharge runs (Fig. 6-1). The planes showed a consistent upstream dip of generally less than 25 deg. As noted earlier, this has been decribed in the field many times (Lane and Carlson, 1954; Rust, 1972a; Davies and Walker, 1974; Hendry, 1976).

This consistency in orientation has both favorable and unfavorable implications. Because of this lack of variation under different flow conditions, data on AB-plane orientation are almost useless in revealing the conditions under which the measured clasts were

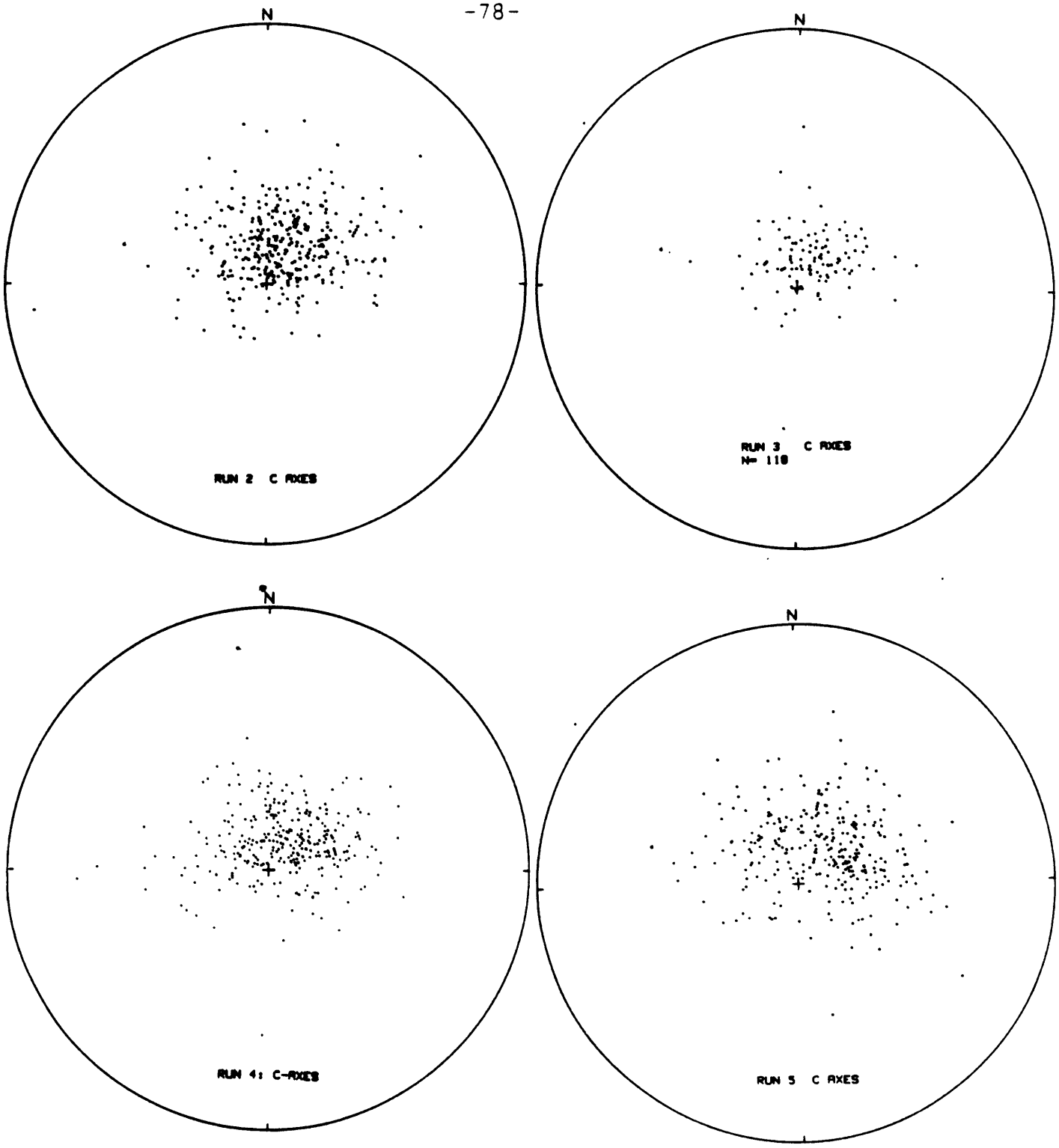

Figure 6-1: Comparision of C-axis Orientations

transported or deposited. However, because the certainty of the AB plane of a clast dipping upstream, the data become a valuable and reliable indicator of paleoflow direction. This is very useful in conglomerates in which sedimentary structures like those found in finer-grained sedimentary beds are rare.

In contrast, the A axis is a poor indicator of flow direction. The data show that the orientations of the A axes were not consistent from run to run, even though the direction of flow obviously remained the same. Attempts to determine the flow direction from A-axis measurements without having any other directional evidence could lead to substantial error in the conclusions. But the fluctuations in A-axis orientations are not random. The breakdown of the orientation measurements by shape and size showed some very definite trends.

The degree of preferred flow-parallel A-axis orientation is directly dependent on the flow strength, increasing with increasing flow strength. Figure 6-2 clearly shows this. Run 3 has an obvious flow-parallel preference, whereas the orientations of Run 5 are display a weak bimodality, with a scatter of orientations from flow-parallel to flow-transverse. In a natural deposit similar to that formed in Run 5, the direction of flow could not be determined. Even in a deposit similar to that of Run 3, it might not be known whether the A axes

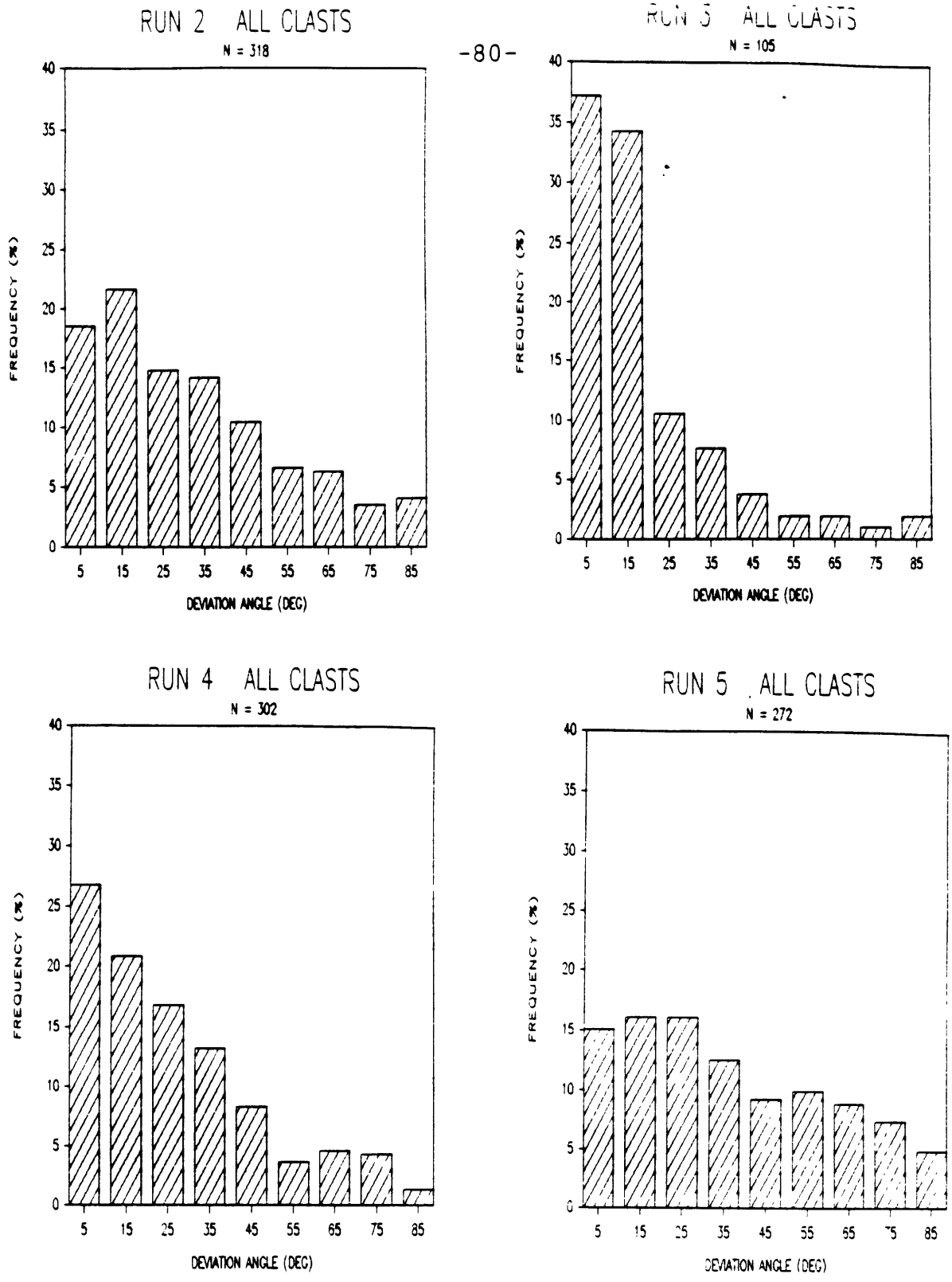

Figure 6-2: Comparision of the Deviation-Angle Frequency Distributions In All The Runs

have a strong preference for an orientation parallel or transverse to the flow, possibly making the determined paleoflow direction 90 deg from the actual flow direction. This study has demonstrated how clast orientation varies with size and shape with a given run (i.e., for given combinations of water discharge, sediment discharge, and deposition rate). Johansson (1965) outlined some of the more important variables, these being clast shape and size, and concentration of clasts in the flow and on the bed. The histograms for each shape group show that the rod-shaped clasts are much more influenced by changes in flow strength than the disks or the blades. In the stronger flows the rods show a very strong preference for being oriented parallel to flow, while in the weaker flows they show a shift towards flow-transverse. The other two shape groups do not show as marked a trend. This would imply that rod-shaped clasts are more indicative of flow strength, given that the direction of flow is known, than are other shapes.

Size, however, did not seem to affect the orientation of clasts in a run. Unrug (1957) stated that the smaller particles assumed an orientation on the bed among the voids left by the larger grains, therefore having a less distinct preferred orientation. This did not seem to be the case in these experiments since no substantial difference was found from one size group to another within

a given run, at least in the coarse part of the size distributions (which was all that was measured in the study).

Concentration of clasts in the flow and on the bed is also an important variable affecting the A-axis orientation. Harms (1975) states that a preferred clast orientation develops when clasts are free to position themselves. This is not possible in higher-concentration flows, such as debris flows, where the clast movement is restricted. Johansson (1963) describes several studies in which it was found that the imbrication of the clasts was better defined, but not the orientation of the A axis. Unrug (1957) points out that a coarse bed (higher concentration of clasts on the bed) causes increased turbulence, resulting in a less regular orientation. In this study the concentration of large clasts in the flow was contolled. The concentration of large clasts on the bed, however, was dependent upon the flow rate, as discussed earlier, and increased with decreasing flow strength. It cannot be determined, therefore, how much of the decrease in preference of flow-parallel orientation can be attributed to the increasing concentration of coarse sediment on the bed.

References

Bagnold, R. A. Experiments on a Gravity Free Dispersion of Large Solid Spheres in a Newtonian Fluid Under Shear. Royal Society Proceedings, 1954, 225, 49-63.

Davies, I. C. and Walker, R. G. Transport and Deposition of Resedimented Conglomerates; The Cap Enrage Formation, Cambro-Ordovician, Gaspe, Quebec. Journal of Sedimentary Petrology, December 1974, 44, 1200-1216.

Fahnestock, R.K. and Haushild, W. L. Flume Studies of the Transport of Pebbles and Cobbles on a Sand Bed. Geological Society of America Bulletin, November 1962, 73, 1431-1436.

Folk, R. L. and Ward, W. C. Brazos River Bar; a Study in the Significance of Grain-size Parameters. Journal of Sedimentary Petrology, 1957, 27, 3-26.

Griffiths, J. C. Scientific Methods in analysis of Sediments. New York:McGraw Hill Co., 1957.

Johansson, C. E. Orientation of Pebbles in Running Water: A Laboratory Study. Geografiska Annaler, 1963, 45, 85-112.

Johansson, C. E. Structural Studies of Sedimentary Deposits. Geografiska Foreningens i Stockholm Forhandlingar, 1965, 87, 3-61.

Kelling, G. and Williams P. F. Flume Studies of the Orientation of Pebbles and Shells. Journal of Geology, May 1967, 75(3), 243-267.

Koster, E. H. Experimental Studies of Coarse-grained Sedimentation. PhD thesis, University of Ottawa, October, 1976.

Krumbein, W. C. Preferred Orientation of Pebbles in Sedimentary Deposits. Journal of Geology, October/November 1939, 47(7), 673-706.

Lane, E. W. and Carlson, E. J. Some Observations on the

Effect of Particle Shape on the Movement of Coarse Sediments. American Geophysical Union Transactions, June 1954, 35(3), 453-462.

Larsson, I. A Graphic Testing Procedure for Point Diagrams. American Journal of Science, 1952, 250, 586-593.

Middleton, G. V. Experimental Studies Related to Problems of Flysch Sedimentation. Flysch Sedimentation in North America, 1970, 7, 253-272.

Rust, B. R. Pebble Orientation in Fluvial Sediments. Journal of Sedimentary Petrology, June 1972, 42(2), 384-388.

Sallenger, A. H. Jr. Inverse Grading and Hydraullic Equivalence in Grain-Flow Deposits. Journal of Sedimentary Petrology, June 1979, 49(2), 553-562.

Sedimentary Petrology Seminar. Gravel Frabic in Wolf Run. Sedimentology, 1965, 4, 273-282.

Unrug, R. Recent Transport and Sedimentation of Gravels in the Dunajec Valley. Acta Geol. Pol., 1957, 7, 217-257.

Walker, R. G. Generalized Facies Models for Resedimented Conglomerates of Turbidite Association. Geological Society of America Bulletin, June 1975, 86, 737-748.

Harms, J.C, Southard, J.B., Spearing, D.R., and Walker, R. G. Depositional Environments as Interpreted from Primary Sedimentary Structures and Stratification Sequences. Lecture notes for Short Course No. 2 sponsored by the Society of Economic Paleontologists and Mineralogists, April, 1975.

Zingg, Th. Beitrag zur Schotteranalyse. Schweizer Min. Petrog., 1935, 15, 39-140.